Jpn. J. Health Phys., **53** (2), 72 ～ 99 (2018) DOI: 10.5453/jhps.53.72

Review (Invited)

Internal Dosimetry —A Review of Progress

Wei Bo Li*[1, #]

（Received on September 30, 2017）
（Accepted on February 3, 2018）

Fifty-five years after discovery of x-rays by Wilhelm Conrad Röntgen in 1895, International Commission on Radiological Protection (ICRP) established a committee on permission internal exposure. Natural and man-made radionuclides can enter human body, cause damage effect and lead to health risk; on the other hand, radionuclides can cure cancers and other non-cancer diseases by irradiating the malignant cells and tissues. The radiation doses delivered to the tissues and organs are inevitable to assess risk or to judge the benefit of application of radiation on humans. In this article, basic methodology for dose assessment of internally deposited radionuclides is reviewed. After brief introduction of interactions and effects of radiation, the biokinetic models developed by ICRP for incorporation of radionuclides in humans are described. Then, the dosimetric formula generalized by ICRP and Committee on Medical Internal Radiation Dose (MIRD) is presented. Treatment of decay products and uncertainty analysis in internal dosimetry are especially addressed. Moreover, applications of internal dosimetry in radiation protection, internal exposure monitoring, radon inhalation dosimetry and nuclear medicine are presented with several calculation examples. At last, the future perspective of internal dosimetry is discussed. In an appendix basic internal dosimetric quantities are provided.

KEY WORDS: internal dosimetry, biokinetic models, computational phantoms, radiation protection, workers, public population, exposure monitoring, nuclear medicine, uncertainty, health risk.

I INTRODUCTION

Internal radiation dosimetry or internal dosimetry[1)] is a complementary research area of external dosimetry in radiation Dosimetry.[2)] Humans and other living beings are living in an environment which is exposed to radiation. Radiation can naturally occur and be produced man-made or by radiation machine. Radionuclides can enter human bodies through various routes, e.g. inhalation, ingestion, injection and through intact skins. This paper concerns only incorporated radionuclides, this means that radionuclides are taken into the human body intentionally or accidentally and irradiate inside the body. Internal dosimetry is a scientific methodology used to measure, calculate, estimate, assay, predict and quantify the radiation energy absorbed by the ionization and excitation of atoms in human tissues as a result of the emission of energetic radiation by internally deposited radionuclides.[3)] The purpose of internal dosimetry may mainly cover the workplace control of exposure, medical intervention and the compliance with standards and regulation.[4)]

According to the exposed population and scenarios, it is convention to classify the internal dosimetry to three main areas: occupational exposure, public exposure and medical exposure. For occupational exposure, the main route of intake is by inhalation, some by ingestion and absorbed by skin through cuts or wounds. For members of the public, the main route of intake is by ingestion in food and drinking water, to some extent by inhalation, however, in accident, for example in Chernobyl and Fukushima nuclear accidents, inhalation may become the main route of intake. In medical application of radionuclides, the main route of intake is by intravenous administration, with a very small part, by oral intake. After entering into the human body, radionuclides can deposit in lungs, alimentary tract and transfer into blood and translocate to other organs and tissues, and some are excreted outside of the body through kidneys and intestine. These dynamic behaviours of radionuclides inside human body are described by biokinetic models.[5, 6)]

For dose assessment, firstly the biokinetic models are needed to model the distribution of radioactivity accumulated in different organs. In the modelling chemical forms of radionuclides are important and should be considered, for example, the chemical toxicity of uranium dominates at enrichments below about 7 to 20%.[7)] It should be noted that the importance of the chemical form in internal dosimetry is owing to the influence on the absorption fraction to blood of radionuclides. Chemical toxicity is beyond the issue of the dose estimation. Then the mean absorbed dose received

*1 Institute of Radiation Protection, Helmholtz Zentrum München-German Research Center for Environmental Health (GmbH); D-85764 Neuherberg, Germany.
Corresponding author; E-mail: wli@helmholtz-muenchen.de

by a target organ or tissue from radionuclides deposited in a source organ or region, the so-called *S* coefficients, are needed to calculate the organ doses. The specific absorbed fractions (SAFs) are commonly calculated based on the absorbed fractions (AFs), which are simulated by performing Monte Carlo radiation transport programs with computational human digital phantoms. The *S* coefficients are evaluated by combining the SAFs and the nuclear decay data. Because the quality of different types of radiation (α, β and γ) of radionuclides makes largely different biological effects and damages to humans in various levels, for example, making DNA breakages, inducing cancers and leading to cell death, the mean absorbed dose in a tissue or organ is weighted by the radiation weighting factors to a new quantity, equivalent dose.

To give a single indicative dose for the whole body, effective dose[8] was proposed by taking into account the radiation sensitivity or susceptibility of different organ or tissue regions. And the effective dose can be calculated by the addition of the organ equivalent doses multiplied by the appropriate tissue weighing factors, which may be evaluated from the human radiation epidemiological data. These dose quantities, e.g. equivalent dose and effective dose are designed for prospective dose assessment for planning and optimization in radiological protection and the absorbed dose should be used for a quantitative assessment of the health risks to environmental radiation exposure. The risk should be considered even in medicine for diagnostic and cancer treatment, for health risk and regulatory decision and radiation risk control. A diagram of general computational method for internal dose assessment is depicted in **Fig. 1**.

It has been found in the early 1940's that the molecular and genetic damages from radiation are initial events for the later biological effects.[9] The need of quantifying radiation dose in the molecular and cellular levels leads to the research area of internal microdosimetry[10] and internal nanodosimetry, for example the application of nanodosimetry for Auger emitters[11] and gold nanoparticles in radiotherapy.[12]

In the entire internal dose assessment as well in monitoring, the parameters used in physics, human anatomy and physiology, the computational methods, like biokinetic modelling and Monte Carlo simulations are subject to a large uncertainty. Some of uncertainties, which may be attributable to measurement techniques and subjective behaviours, can be reduced; some are aroused from the natural variability of humans and can be quantified but are generally difficult to be reduced. Therefore uncertainty analysis in internal dosimetry is gradually attracting attention for the need of reliability in risk estimation.

In summary, in this paper, the basic physical, chemical and biological effects of radiation are briefly introduced. The state-of-the-art methodologies for estimating internal radiation doses are mainly reviewed. Some applications and calculation examples of internal dosimetry in radiation protection, internal monitoring and in medicine are presented. Readers may find a starting point of internal dosimetry in the present review, follow the leitmotiv and participate in this continuously

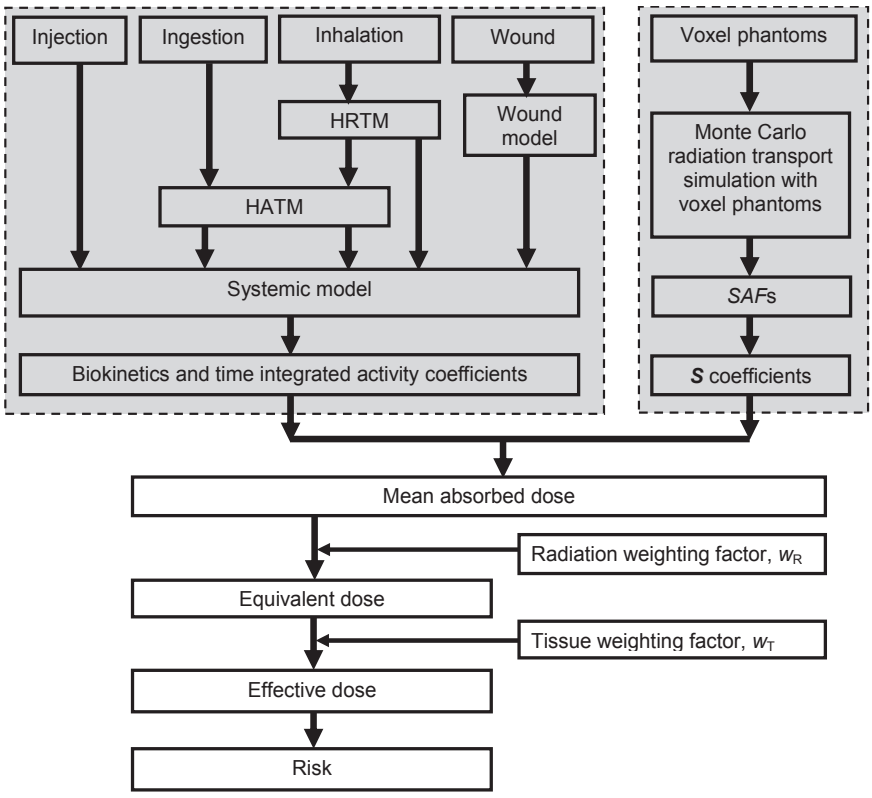

Fig. 1 General computational diagram of internal dose assessment.

developing research field.

II PHYSICAL AND BIOLOGICAL FOUNDATIONS

Physical dose is an indicator to quantify the response relation of radiation and biological effect. The interactions of radiation with biological material in different levels can help to understand the causation and mechanism of radiation biological damages.

1. Interaction of radiation with living tissues

In internal dosimetry, α, β and γ radiations are more relevant than neutrons, protons and heavy ions. α-particle is charged heavy particle and is not very penetrating. Therefore α-particle is important in cellular level in lungs and other organs especially through inhalation. In biological material, energy transfer of α-particle occurs preliminarily through excitations and ionizations and is described by stopping power which is defined average energy loss per unit distance along its path. However, the lost energy by α-particle transfers to the secondary radiation, like electrons and photons which penetrate to distance from the particle tracks. To measure the energy that is laid down close to the particle tracks, the quantity linear energy transfer (LET or L) is introduced by excluding the energy carried away by photons and energetic electrons. L can be quantified with a limit L_Δ, where energy above Δ will not be accounted, or without limit L_∞, in this case, it equals to stopping power.[13)]

Energy of electron is mainly transferred to matter through interaction of electric field of moving electrons with that of electron bound in the medium. The interactions lead to electronic ionizations and ionizations and the slow down electron with residual energy lower than 10 eV will lose energy by direct excitation of rotational, translational or vibrational modes of molecular affected. Elastic, excitation and ionization cross sections for electrons were calculated for liquid water and DNA molecular moiety to mimic the interactions of electrons in biological tissues.[14, 15)]

Photons interact with molecule in three main processes: photoelectric effect, Compton scattering and electron-positron pair production event. The fourth process, elastic photon interaction, also Rayleigh scattering is important at low energy below 100 keV, and this event changes the direction of photon and the energy deposition of location of the next inelastic event.[16, 17)] The cross sections for the processes in liquid water and other materials are well calculated and available to quantify the energy deposition in the biological materials.[18)]

Based on the cross sections of radiation transport in biological material, the energy deposition and the physical dose such as absorbed dose,[13)] D, in materials can be quantified. Mean absorbed dose[19)] in a tissue or organ, D_T was defined as a physical dose in human body. Because the different radiation types have different qualities on organs and tissues, the absorbed dose was weighted by radiation weighting factor to obtain the equivalent dose,[19)] H_T in a tissue or organ. However, different tissues or organs in human body react to radiation differently, which was known as susceptibility. The effective dose,[19)] E which is a weighted equivalent dose by tissue weighting factor w_T for target tissue T, is defined to represent the whole body dose for radiological protection. These three essential quantities can be found in the appendix.

2. Radiation chemical and biological effects

After completion of the physical interaction of radiation in liquid water, different new chemical species are produced and will diffuse in water and interact each other and with DNA and lead to the indirect damage in contract to the direct radiation effect induced by physical energy deposition. Preliminary, the sub-excitation electrons, e_{sub}; ionized water molecules, H_2O^+; excitation states: $\widetilde{A}^1B_1$ and $\widetilde{B}^1A_1$; Rydberg states; diffuse bands and dissociative excitations are produced. It has been conjectured that ionized water molecules react immediately following the scheme on the time scale 10^{-14} s:

$$H_2O^+ + H_2O \rightarrow H_3O^+ + {}^{\cdot}OH$$

The excited water molecules are assumed either to relax, auto-ionize or dissociate in different possible ways and produce other chemical species: ${}^{\cdot}OH$, H_3O^+, $H^{\cdot}$, H_2, e_{aq}^-, OH^- and H_2O_2. These radicals diffuse in water in diffusive Brownian motion.[20, 21)] It is assumed that ${}^{\cdot}OH$ radicals interact with nucleotides, sugar-phosphate moieties and base, contributing to DNA lesion complexity; however, the hydroxyl radicals can be scavenged in the cytoplasm. Other than damage to DNA, radiation can destroy cell membrane and leads to cell deaths.[22)] Mitochondrion in cytoplasm is also regarded as a target for cell death of radiation.[23)]

The somatic effects are generally classified to two group (1) deterministic effects (harmful tissue reactions) due in large part to the killing or malfunction of cells following high doses; and (2) stochastic effects, i.e., cancer and heritable effects involving either cancer development in exposed individuals owing to mutation of somatic cells or heritable disease in their offspring owing to mutation of reproductive (germ) cells.[19, 24)]

Deterministic effects can generally be characterized by a threshold of radiation dose. At this threshold dose, the radiation damage (serious malfunction or death) of a critical population of cells in a given tissue can be sustained before injury is expressed in a clinically relevant form. Above the threshold dose the severity of the injury, including impairment of the capacity for tissue recovery, increases with dose.

For stochastic effects, it is in debate, if there is a dose threshold, say less than 100 mSv, to induce a cancer. Risk model is used to quantify the health risk of low-dose radiation. Several concepts, like relative biological effectiveness (RBE),[25)] radiation weighting factor (w_R) and dose and dose rate effectiveness factor (DDREF)[26)] are used to link the molecular effects to tissue and somatic effects. The linear-non-threshold (LNT) model has been recommended in the radiation protection practice, however, more researchers and organizations recently convicted to this model with arguments that the model is inconsistent with radiation biological and experimental data.[27–29)] The debate needs the molecular radiation biological investigations like, DNA damages, chromosome aberrations, cellular deaths or transformation,

and extension to somatic effects.

Taking into account all the processes of radiation interactions in human body, radiation risk can be estimated by different models, such as (a) direct estimates of risk from a large population, (b) mathematical models, (c) biologically based risk models and (d) empirically based risk models with anticipated uncertainties.[30–32]

III BIOKINETIC MODELS

Radionuclides can accidentally and intentionally enter human body through various incorporation routes, e.g. inhalation, ingestion, injection, transdermal resorption, wound, instillation and other orifice of the body, especially with intentional application of radioactive medicaments in nuclear medical diagnostics and therapy.[33–35] The uptake of radionuclides in the blood through respiratory tract or alimentary tract can further be continuously transferred and distributed, like the radionuclides directly injected into blood, to other organs and tissues. Incorporated radionuclides can be eliminated or excreted through kidneys by urine, through alimentary tract by faeces, through exhalation and through skin by sweat, excretion in nails and hair. The intake and uptake and transfer and distribution, elimination and excretion are generally described as biokinetics of incorporated radionuclides in human body and are illustrated in **Fig. 2**.

The concept of biokinetics was derived from Greek words bio (life) and kinetics (transport).[6] In the earlier publications of ICRP,[36, 37] the concept of metabolism is used which is more about the chemical and physical changes of the substances.[6] The biokinetic model was used by ICRP from its publication 56[38] and can be described in a form of compartmental model.[5] Basically the biokinetic model can be mathematically described in a system of coupled differential equations with first-order or higher-order.[39–41]

To quantitatively calculate the internal doses, the biokinetic information of incorporated radionuclides must be determined first. Directly quantifying the distribution and retention of radionuclides in human body is experimentally unpractical and challenging. However, these data are basis for setup of biokinetic model and calculating the cumulated radioactivity in human body for dose estimation. The biokinetic data were retrieved from laboratory animal experiments, sometimes from severe sick patients, accidental human data or in less extent from studies with healthy subjects.[36, 42]

Generally, a center compartment representing blood was connected to each organ and tissue. Gastrointestinal tract model, now alimentary tract model and lung model, now respiratory tract model were separately developed to describe the intake of radionuclides through ingestion and inhalation. The systemic biokinetic models, the alimentary models and the respiratory model can be coupled and connected through human physiological metabolism of materials in human body, like absorption of small intestine and clearance and absorption in lungs.

1. Systemic biokinetic models

The transfer and retention of radionuclides through blood to internal organs and tissues are described as systemic biokinetic models. For each element, a systemic biokinetic model is developed based on the human data available from environmental, accidental or medical exposure, and to a greater extent from experimental animals. The principle of building a systemic biokinetic model is to set a compartment representing an organ or tissue region, sometimes to use several compartments for one organ or tissue region, if the activity in the sub-region is available, the connection of the

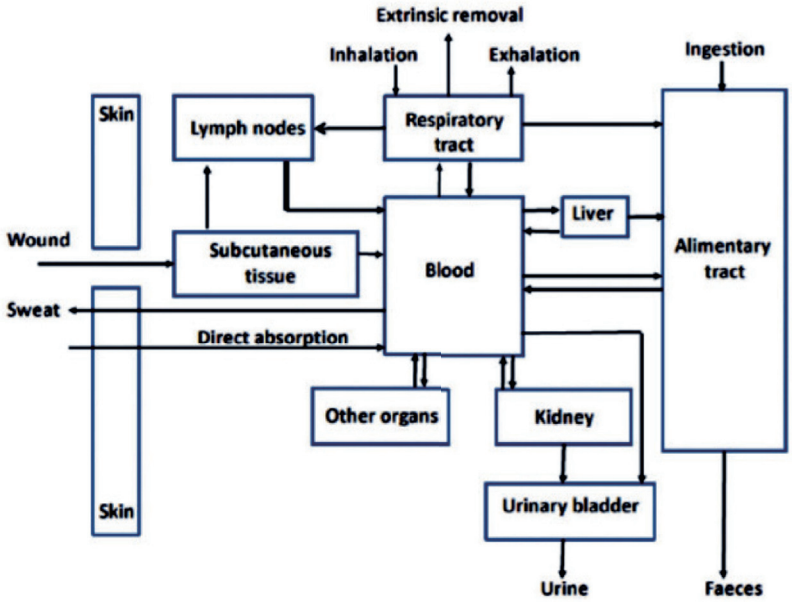

Fig. 2 Generic biokinetics of incorporated radionuclides in human body predicted by a compartmental model.[63] This picture is adopted from Fig. 3.1 of ICRP Publication 130 under the permission granted by ICRP on 27 January 2018.

organ or tissue to blood is human physiological based,[43] a compartment called "other" is setup to represent the activity which is not distributed to a certain organ or tissue, and this compartment comprises all the organs not explicitly present in the biokinetic model.

In the early times and as well in nuclear medicine, a multiple-term of exponential function was used to fit the measured activity in organs without knowing the physiological knowledge.[36, 37] From its publication 56[38], ICRP applied physiological based biokinetic models to determine the retention and excretion of incorporated radionuclides.[38, 44, 45] The systemic biokinetic model usually includes a central compartment representing for blood and/or plasma. In this compartment, depending on the nuclide a sub-compartment representing red blood cell or just a sub-compartment representing the process that nuclide was bound to some protein in the blood, was introduced.

The soft tissues, in one compartment or sometimes in three sub-compartments, rapid turnover (ST0), intermediate turnover (ST1) and slow turnover (ST2), are connected to the blood compartment. For many nuclides, certain explicit organs are presented in the systemic model, for example, brain, heart wall, pancreases and spleen and lung tissues are connected directly to blood, the remainder organs or tissues which are not present in the model are assumed to be a part of other soft tissues (ST0, ST1 and ST2). A skeleton compartment is connected to blood for the bone seeking nuclides. In the skeleton compartment, often six sub-compartments, cortical and trabecular surface, cortical and trabecular deep and shallow volumes are assumed; for some elements, e.g. thorium, cortical and trabecular marrow are added and the cortical and trabecular deep and shallow volumes are reduced to only volumes. For many nuclides, compartments liver 1 and liver 2 are used to model the materials which are transferred through the whole liver to the gastrointestinal tract, now the alimentary tract, and are further excreted outside the body by faeces. At this excretion route, radionuclides can be transferred directly from blood to alimentary wall and excreted to faeces.

Mechanism of urine formation and excretion and its compartmental model is generally a part of the systemic biokinetic model. The urinary excretion model comprises of a compartment of other kidneys tissue for exchange of nuclide to blood, a urinary path for pathway of nuclide to urinary bladder. For example, in **Fig. 3** the mechanism of urine formation is transformed to a compartmental model for urinary excretion of strontium.[46] For some nuclides, certain explicit compartments are presented in the systemic model for excretion: for example in biokinetic model of Cs,[47] the skin as an excretion path to sweat; hair as a compartment in systemic biokinetic model of Pb for excretion path. Hair and nails can be added to the ICRP biokinetic uranium model to describe the measured data with a sharing excretion pathway through hair in addition to the urinary excretion.[48]

The MIRD Committee developed independently a dynamic kidney model to drive the urinary excretion of the radiopharmaceuticals for patients undergoing diagnostics and therapy in nuclear medicine.[49]

2. Human alimentary tract model

The new human alimentary tract model (HATM)[50] (**Fig. 4B**) was developed based on the gastrointestinal tract (GIT) model[37] (**Fig. 4A**) which was established in 1979. The GIT model was developed on the basis of data reviewed by Eve[51] in 1966, it was used to calculate the dose for workers from both ingestion and inhalation of radionuclides. The GIT model took into account of transit of ingested materials through four

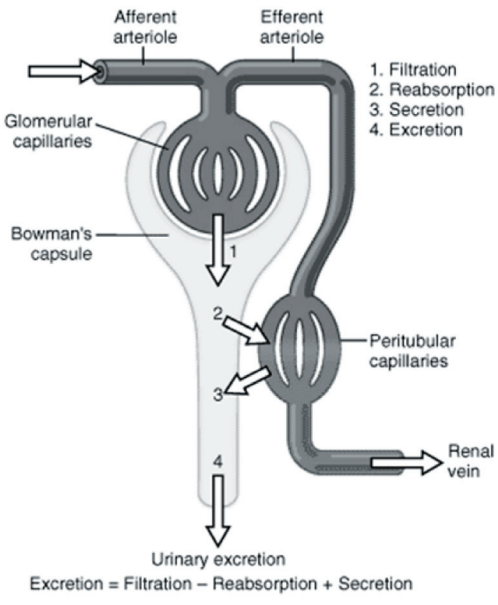

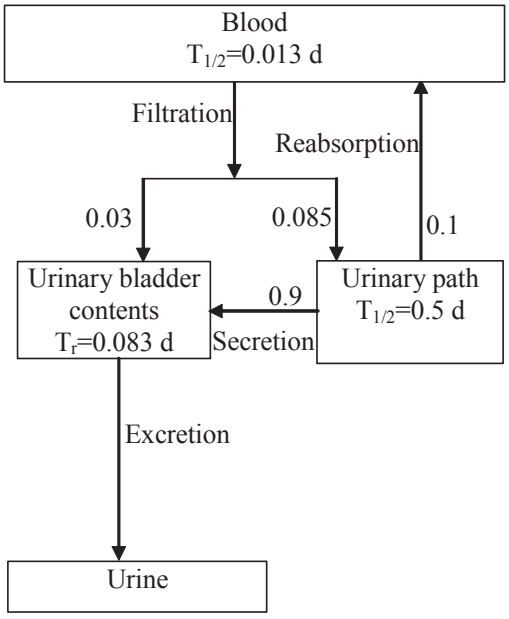

Fig. 3 Urinary excretion compartmental model, used for fitting the measured human data of strontium.[46] The picture of the left panel is adopted from Fig. 26-8 of Guyton and Hall[43] under the permission granted by Elsevier Ltd. on 20 July 2018.

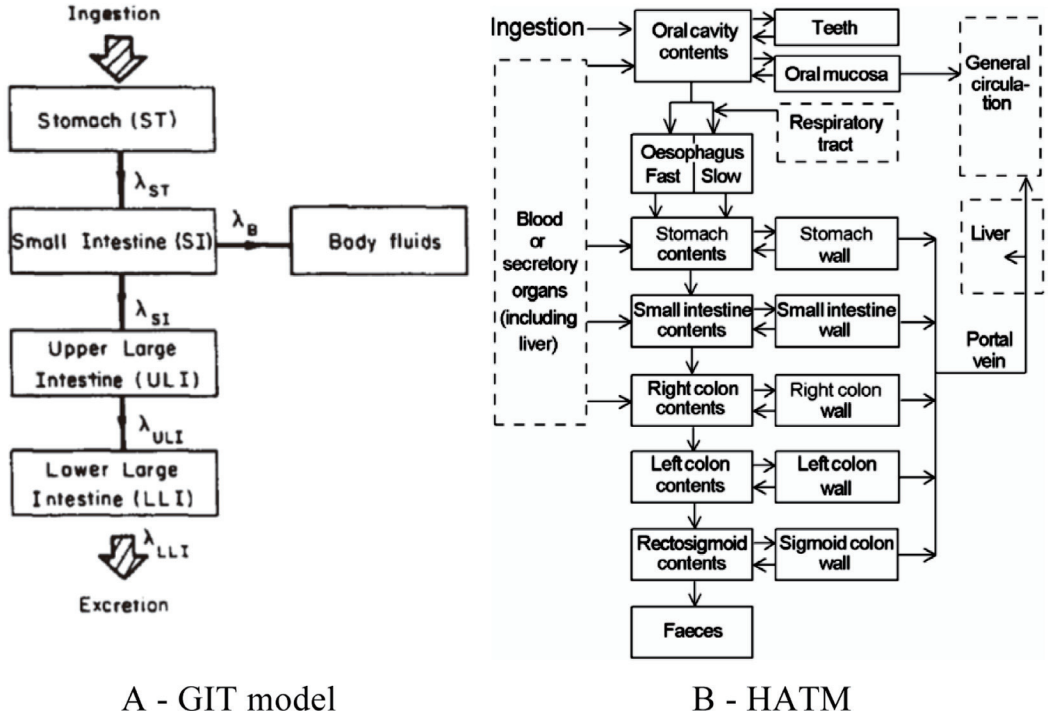

Fig. 4 Gastrointestinal tract (GIT) model[37] (A) and human alimentary tract model (HATM)[50] (B) developed by ICRP. The dashed boxes in B show the compartments outside of the alimentary tract and they are connected to the HATM and GIT model. The picture (A) is adopted from Fig. 6.1 of ICRP Publication 30 Part 1 and the picture (B) is from Fig. 3.6 of ICRP Publication 130 under the permission granted by ICRP on 27 January 2018.

regions of the alimentary tract: stomach, small intestine, upper large intestine and lower large intestinal. The transfer rate of λ_B can be estimated from the so called f_1 value, which is defined as the absorption fraction of radionuclide to blood:

$$\frac{\lambda_B}{\lambda_{SI}+\lambda_B}=f_1 \text{ and } \frac{f_1\lambda_{SI}}{1-f_1}=\lambda_B.$$

This GIT compartmental model did not include feedback and can be analytically solved as Eq.(1) by a system of differential equation:[37, 52]

$$q_i(t)=\left[(\Pi_{k=1}^{i-1}\lambda_{(k,k+1)})\sum_{\substack{p=1\\p\neq k}}^{i}\frac{q_1(0)e^{-\lambda_k t}}{\Pi_{k=1}^{i-1}\lambda_p-\lambda_k}\right], \quad (1)$$

where

$\Pi_{i=m}^{n} a_i = a_m \times a_{m+1} \times \ldots a_n$ if $n \geq m$ and

$\Pi_{i=m}^{n} = 1$ if $n < m$.

A considerable data has become available on the transit of materials through the different regions of the gut since the development of the GIT model. These data provide the differences between solid and liquid phases, age and gender-related differences; Furthermore, the ICRP 1990 recommendation revised radiation risks, especially for specific risk estimates for cancer of the oesophagus, stomach and colon. Therefore, a new alimentary model is needed to include oesophagus, stomach and colon as specified target tissues.[50]

The new HATM was developed and compartments in mouth region, oral cavity contents, teeth, oral mucosa and oesophagus in two compartments were added before the materials transfer to stomach which was split to two compartments: contents and wall. The upper and lower large intestines were extended to right, left and rectosigmoid part each with contents and wall compartments (**Fig. 4B**). Radionuclides can be transferred to circulation system in mouth and radionuclides as contents will more realistically be transferred through intestinal and colon walls to circulation system and radionuclides can be transferred back to alimentary tract. However, it became more complicated to solve the complete compartmental models and the new defined alimentary tract transfer factor f_A should be the sum of fraction from stomach, small intestine, right and left colon and rectosigmoid: $f_A = \Sigma f_i$ with f_i for absorbed fraction in all of the regions of the alimentary tract: stomach (ST), small intestine (SI), right colon (RC), left colon (LC) and sigmoid (S) (see **Fig. 4B**). Because of the lack of data, in practice, it is assumed that materials are absorbed mainly in SI region: $f_A = f_{SI}$. However, if transfer data in the alimentary regions are available, they should be used in the biokinetic modelling. Transfer coefficients (per day) for the movement of alimentary tract content between regions are indicated in **Table 1**.

3. Human respiratory tract model

In its Publication 2, ICRP recommended a very simple

Table 1 Transfer coefficients (per day) for the movement of alimentary tract between regions.[50)]

Region	Age 3 moths	Age 1 year	Age 5–15 years	Adult male	Adult female
Mouth					
Solids		5,760	5,760	5,760	5,760
Liquids	43,200	43,200	43,200	43,200	43,200
Total diet	43,200	7,200	7,200	7,200	7,200
Oesophagus (fast)					
Solids		10,800	10,800	10,800	10,800
Liquids	21,600	17,280	17,280	17,280	17,280
Total diet	21,600	12,343	12,343	12,343	12,343
Oesophagus (slow)					
Solids		1,920	1,920	1,920	1,920
Liquids	2,880	2,880	2,880	2,880	2,880
Total diet	2,880	2,160	2,160	2,160	2,160
Mouth					
Solids		19.2	19.2	19.2	13.71
Caloric liquids	19.2	32	32	32	24
Non-caloric liquids	144	48	48	48	48
Total diet	19.2	20.57	20.57	20.57	15.16
Small intestine	6	6	6	6	6
Right colon	3	2.4	2.182	2	1.5
Left colon	3	2.4	2.182	2	1.5
Rectosigmoid	2	2	2	2	1.5

(This table was reproduced after the Table 6.6 of ICRP Publication 100)

model to descript the inhaled particles in human respiratory tract: 50% of an inhaled aerosol would be deposited in the upper respiratory tract, 25% would be exhaled, and 25% would be retained in the lungs.[42)] In 1966, a Task Group on Lung Dynamics (TGLD) published a revised lung model,[53)] it was used in dose calculation for occupational workers in ICRP Publication 30 series.[37, 54–60)] In this model, the respiratory system is divided into three regions; the nasal passage (N-P), the trachea and bronchial tree (T-B) and the pulmonary parenchyma (P). The depositions in different regions were described by three fractional deposition parameters: $D_{N\text{-}P}$, $D_{T\text{-}B}$ and D_P. The aerodynamic property of aerosol distribution with activity median aerodynamic diameter (AMAD) of aerosol was used. For the clearance of particles from the lungs, the materials were classified as D, W and Y. **Fig. 5** showed the compartmental lung model and the related parameters.

In 1994, ICRP revised the ICRP 30 lung model and published a new human respiratory tract model (HRTM).[61)] This model improved the respiratory model in many aspects. This model is a compartmental model based on the morphometric and anatomic characteristics of the human lung (**Fig. 6A**) and considered human respiratory tract as four anatomic regions: the extrathoracic region (ET), the bronchial region (BB), the bronchiolar region (bb) and the alveolar-interstitial region (AI). The model provides a set of age- and sex-dependent physiological parameters. This model included a deposition model, a clearance model and an absorption model.

		Class					
		D		W		Y	
Region	Compartment	T day	F	T day	F	T day	F
N–P	a	0.01	0.5	0.01	0.1	0.01	0.01
(D_{N-P} = 0.30)	b	0.01	0.5	0.40	0.9	0.40	0.99
T–B	c	0.01	0.95	0.01	0.5	0.01	0.01
(D_{T-B} = 0.08)	d	0.2	0.05	0.2	0.5	0.2	0.99
	e	0.5	0.8	50	0.15	500	0.05
P	f	n.a.	n.a.	1.0	0.4	1.0	0.4
(D_P = 0.25)	g	n.a.	n.a.	50	0.4	500	0.4
	h	0.5	0.2	50	0.05	500	0.15
L	i	0.5	1.0	50	1.0	1 000	0.9
	j	n.a.	n.a.	n.a.	n.a.	∞	0.1

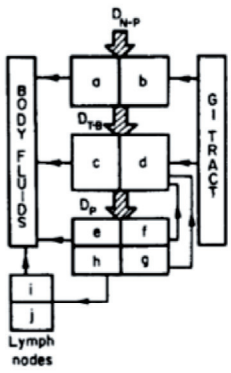

Fig. 5 A mathematical model used to describe clearance from respiratory system in ICRP Publication 30.[37)] This picture is adopted from Fig. 5.2 of ICRP Publication 30 Part 1 under the permission granted by ICRP on 27 January 2018.

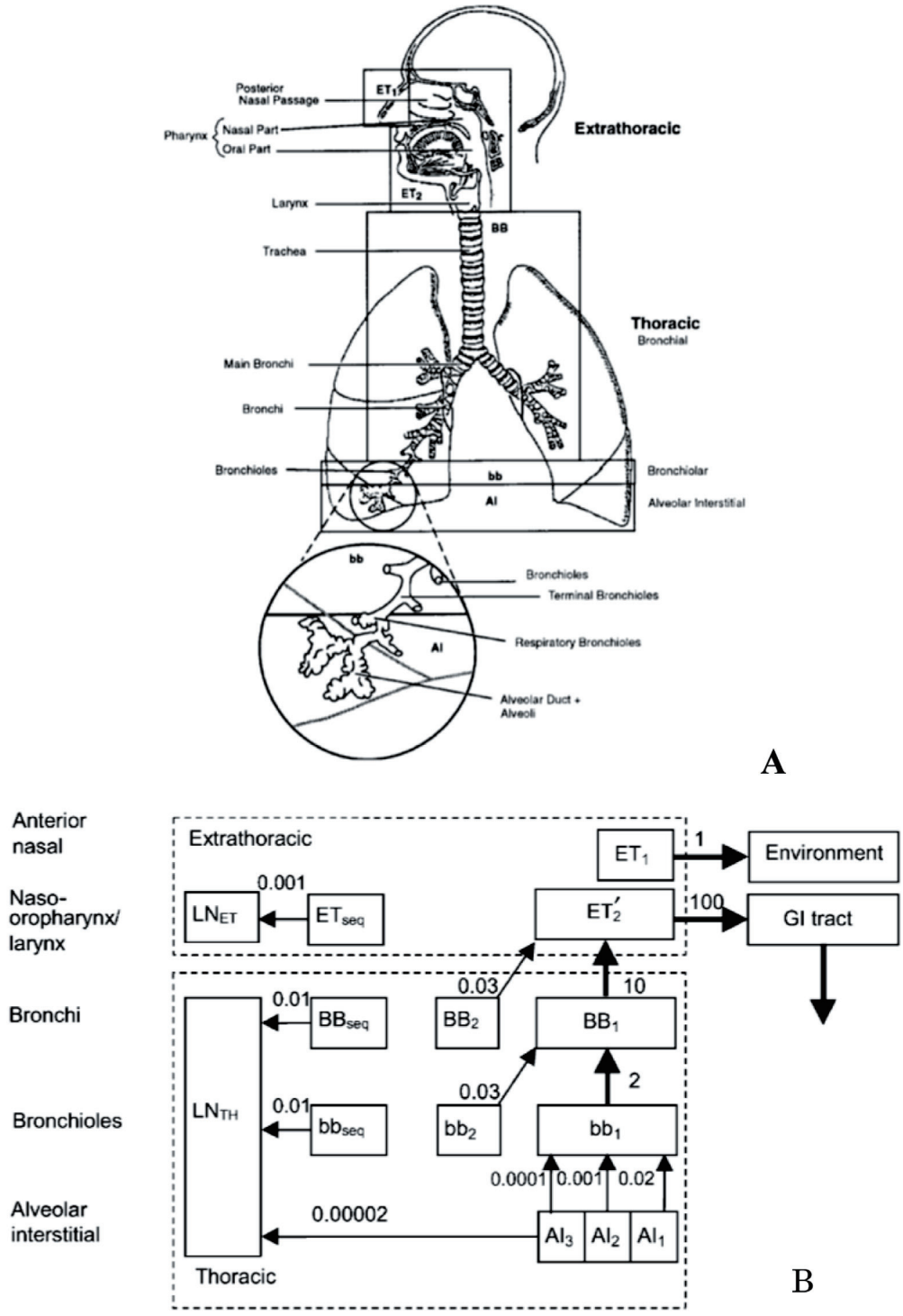

Fig. 6 Respiratory tract regions (A) in HRTM and compartmental model (B) representing particle transport from each respiratory tract regions.[61] The picture (A) is adopted from Fig. 3.2 and the picture (B) is from Fig. A.1 of ICRP Publication 130 under the permission granted by ICRP on 27 January 2018.

In the deposition model, three main mechanisms of airborne particles in the respiratory tract were considered to determine the activities: gravitational sedimentation, inertial impaction and Brownian motion or diffusion.[62] Analytical formulas are given for determination of regional deposition fraction in airways. The clearance model is a compartmental model (**Fig. 6B**) based on anatomic regions with transfer rates among compartments; the radionuclides accumulated in different regions will be transferred to blood by an absorption model (**Fig. 7**). In the biokinetic modelling, model (b) is practically

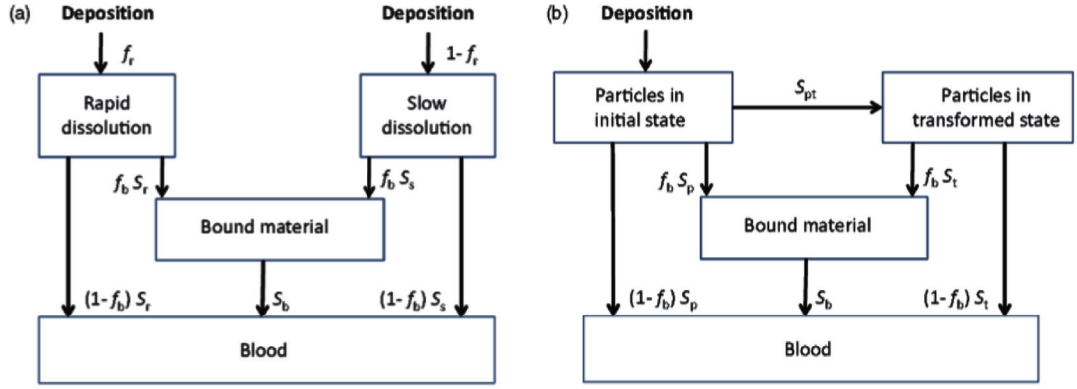

Fig. 7 Two alternative compartmental models for time-dependent absorption into blood reported by ICRP Publication 130.[63] In model (a) a fraction of the deposit is initially assigned to the compartment labelled 'rapid dissolution', and the rest of the deposit is initially assigned to the compartment labelled 'slow dissolution'. In model (b), all the deposit is initially assigned to the compartment labelled 'particles in initial state', and material in the compartment labelled 'particles in transformed state' is subject to particle transport at the same rate as material in the compartment labelled 'particles in initial state'. It may be noted that any time-dependent dissolution behaviour that can be represented using the model shown in model (a) can also be represented by the model shown in model (b) with a suitable choice of parameter values. These two pictures are adopted from Fig. 3.5 of ICRP Publication 130 under the permission granted by ICRP on 27 January 2018.

implanted in the compartmental model. For all elements, default values of parameters in ICRP Publication 66 were revised and are recommended, according to whether the absorption is considered to be fast (Type F), moderate (Type M), or slow (Type S). For gases or vapours, instantaneous uptake into blood may be recommended [Type V (very fast)].[63] Where information was available, specific parameter values, which were derived from experimental data, are summarised in the inhalation sections of each element in the new ICRP publication series-Occupational Intakes of Radionuclides (OIR).[47, 63] Furthermore, it is necessary to mention that the structure of HRTM developed in ICRP Publication 66[61] has been modified in ICRP OIR Part 1[63] in view of experience and new information, for example, three compartments of alveolar interstitial (AI1, AI2, AI3) were merged to one compartment alveolar (ALV).

For gases and vapours a model is provided, three classes of gases uptake pattern; insoluble and non-reaction gases SR-0, soluble or reaction gases and vapours (SR-1) and soluble and reaction gases and vapours (SR-2) were recommended, so that the deposition of radon gas and other gases can be calculated. Based on this model for gases and vapours, Leggett et al.[64] proposed a new model for radon and other noble gases. In the OIR series, the general defaults for gases and vapours are 100% total deposition in the respiratory tract (regional deposition: 20% ET2, 10% BB, 20% bb, and 50% AI) with Type F absorption. This classification is somewhat different from that recommended in Publication 66[61].

4. Wound models

To assess the dosimetry of radionuclides that enter the human body through wound, ICRP and NCRP jointly developed a biokinetic model for determining the retention and excretion of internally deposited radionuclides through wound. Actually the wound model is very similar to the systemic biokinetic models, however, the connection of wound model with and to other biokinetic models is somehow very specific due to the chemical characters of radionuclides or the wound property. The NCRP wound model (**Fig. 8**) consists of seven compartments. Five of these compartments (fragment, soluble, colloid & intermediate state (CIS), particles, aggregates & bound state (PABS), and transport particles & aggregates (TPA)) comprise the wound site and two (blood and lymph nodes) receive materials leaving the wound sites and enter the blood. The five-compartment wound site is considered to be relatively tissue insensitive and, therefore, independent of the anatomic location of the wound.[65]

Depending on the different injure scenarios and radionuclide chemical states, different accidental inject route is applied, as indicated in **Fig. 8**. For example, for fragment forms of radionuclides, the model of injection to fragmentation compartment is used and the other injection routes will not be used. However, if the contaminating material consists of a mixture of forms, then all the relevant portions of the model will need to be used. Readers can find an example[66] of applying this wound model which is coupled to uranium systemic biokinetic model for assessing internal radiation doses after contamination of depleted uranium.

5. Model for skins

Some radionuclides, tritium oxide as liquid or vapour and iodine as vapour or in solution can be absorbed by the intact skin. The tritiated organic compounds can be directly absorbed and is instantaneously distributed within whole body water like that after inhalation or ingestion. In addition to calculate the dose to the area of skin, the dose to other inner organs and tissues needs to be considered. ICRP Publication 60 has recommended that for skin contamination

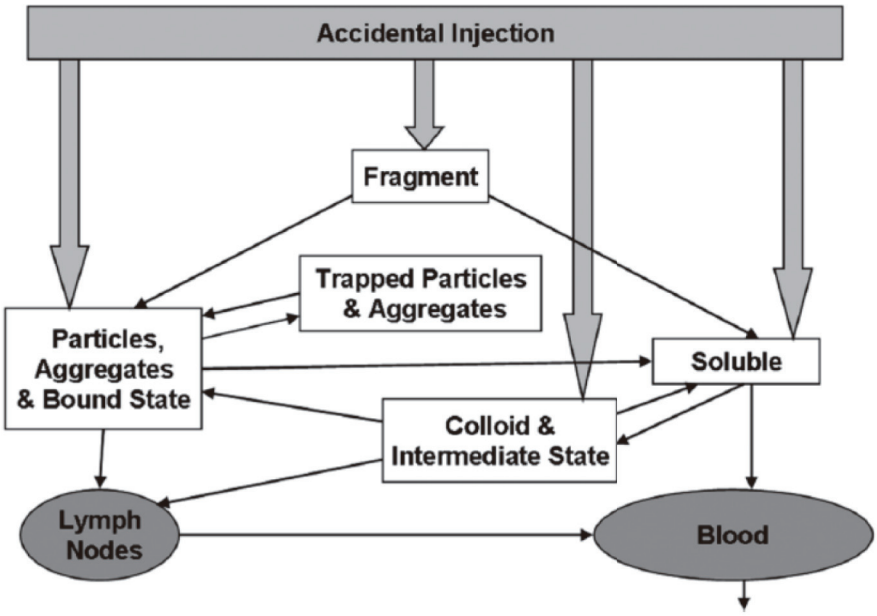

Fig. 8 Wound model developed by NCRP and ICRP.[65] This picture is adopted from Fig. 3.7 of ICRP Publication 130 under the permission granted by ICRP on 27 January 2018.

doses should be calculated to sensitive cells, assuming to be at a depth of 70 μm. In some cases, the inhalation dose coefficient of airborne HTO vapour can be used for intact skin contamination. There is no specific model developed by ICRP for skin contamination. Traub et al.[67] developed a computer code VARSKIN for the calculation of tissue dose at various depths as the result of skin contamination. The contamination was assumed to be a point or an infinitely thin disk source located directly on the skin. Now the computer code has been updated by US NRC to Version 5.[68] Five different predefined source configurations are available in VARSKIN 5 to allow simulations of point, disk, cylinder, sphere, and slab sources. It included an enhanced photon dosimetry model, as well as models to account for air gap and cover materials for photon dosimetry and predicts beta dosimetry in shallow skin targets.[68]

Recently, the uptake of radon through skin was evaluated by Sakoda et al.[69] They added to the latest biokinetic model for noble gases an uptake path via the skin using the skin permeability coefficient as parameter.

6. Generic biokinetic models for incorporated radionuclides

To assess the distribution and excretion of incorporated radionuclides by injection, systemic biokinetic model is used. The systemic model is coupled to the HATM to set up a biokinetic model for describing the behaviour of radionuclides in human body after ingestion. For the inhalation route, the combined systemic and alimentary tract models are combined to the HRTM through the clearance from lung to the blood and partly to oesophagus and further to blood in stomach wall and small intestinal or colon walls. **Fig. 9** shows a generic biokinetic model for incorporated radionuclide with the GIT model and systemic biokinetic model of uranium. **Fig. 10** shows a generic biokinetic compartmental model for depleted uranium after inhalation which combines the systemic biokinetic model of uranium, the HRTM and the HATM.[66] Replacing the systemic biokinetic model of uranium with models of any other elements, one can build up a generic biokinetic model to predict the behaviour of radionuclides in human body. A bound state in the HRTM for some element, e.g. plutonium should be considered.

If we assume that, in the beginning, numbers of atoms of radionuclide in decay chain with member n ($n = 1, 2, \ldots N$, with $n = 1$ as parent radionuclide) was inhaled in compartment, i, which is connected to other compartment, j. The biokinetic behaviour of the atoms of nuclide n in compartment i at time t, $q_{i,n}(t)$ can be descripted by a system of first-order linear differential equations in Eq.(2):

$$\frac{dq_{i,n}(t)}{dt} = I_{i,n}(t) + \sum_{\substack{j=1 \\ j \neq i}}^{J} q_{j,n}(t)\, k_{i,j,n} - q_{i,n}(t) \sum_{\substack{j=1 \\ j \neq i}}^{J} (k_{i,j,n} + \lambda_n) + \sum_{m=1}^{n-1} q_{i,m}(t)\, \beta_{n,m}\, \lambda_n \qquad (2)$$

where: $\dot{I}_{i,n}(t)$ is the input flow rate to compartment i of nuclide of decay member n from the environment. $k_{i,j,n}$ is the transfer rate from compartment j to i for nuclide member n; λ_n is the physical decay constant of radionuclide n. J is the number of compartments which are connected to compartment i. $q_{i,m}(t)$ is the atoms of nuclide n that ingrowths in compartment i at time t from nuclide member m in decay chain; $\beta_{n,m}$ is the branching fraction of the chain member m that decays to member n. The decay data of radionuclides can be retrieved from ICRP Publication 107[70] and the accompanying CD.

It is noted that in the biokinetic modelling, those are the

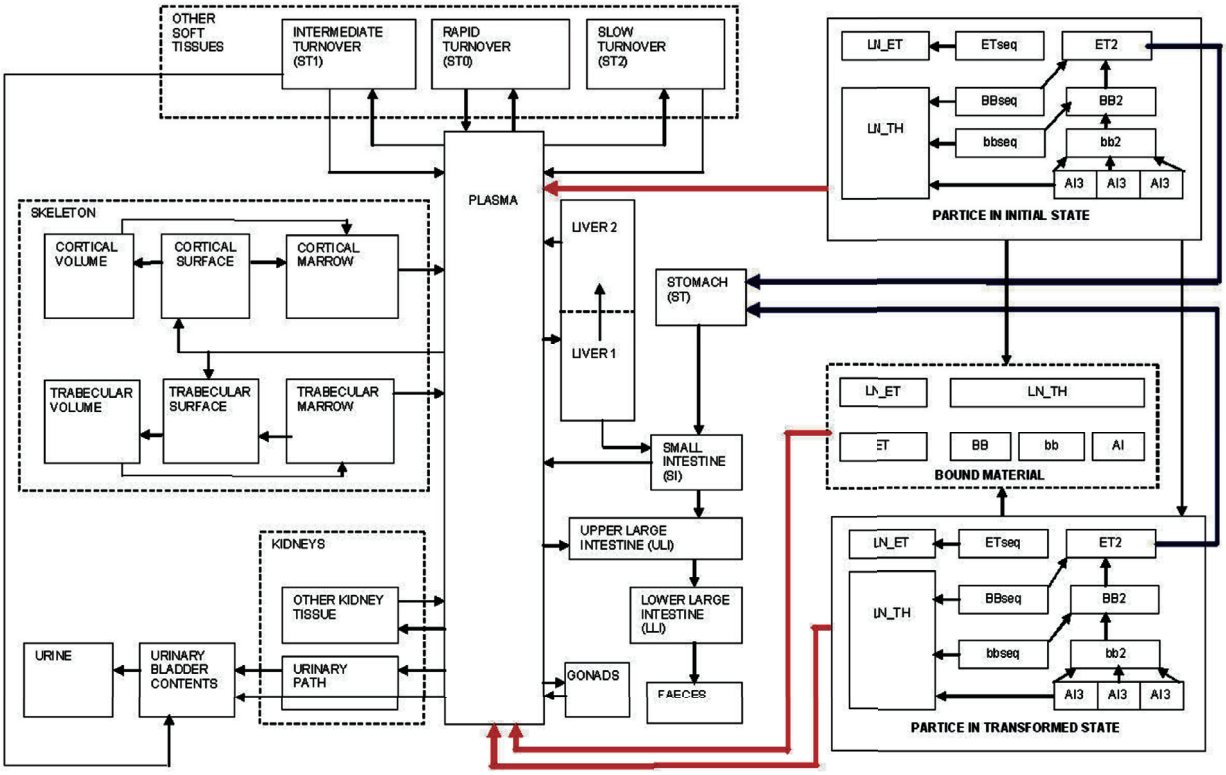

Fig. 9 A biokinetic model for incorporated radionuclide of uranium. For uranium, the bound material state is not used. The systemic biokinetic model of uranium can be replaced by other systemic biokinetic models and the whole structure of the compartmental model can be used to represent a generic biokinetic model for incorporated radionuclides.

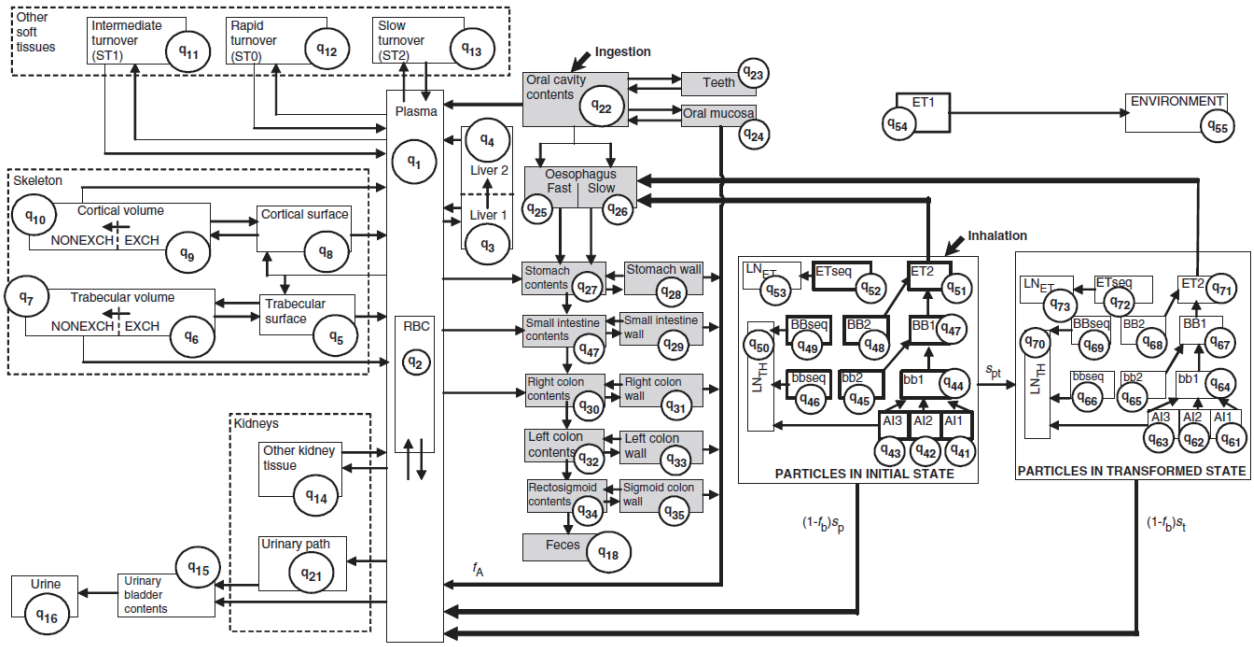

Fig. 10 Biokinetic compartmental model for uranium after inhalation.[66] It combines the systemic biokinetic model of uranium, the HRTM with HATM.

atoms that are transferred between compartments and follow the law of conservation of mass. The complete system of first order linear differential equation shown in Eq.(2) can be solved by initial conditions by numerical methods. The results, number of atoms in compartments at different time, $N(t)$, can be converted to radioactivity at time t, $A(t)$ by the relationship $A(t) = \lambda N(t)$.

IV DOSIMETRIC MODELS

A naive concept for estimating absorbed dose in human body could be preliminarily formulated as the quotient of the decay energy deposited of the incorporated radionuclides in the body and the mass of the body. However, the incorporated radionuclide transfers to different organ and tissues through blood circulation system and can be excreted through kidney in urine and alimentary tract in faeces and consequently eliminated out of the human body. Radiation can penetrate organs to outside the body, so that not all decay energies deposit inside body. Furthermore, radionuclides distribute heterogeneously in various organ and tissues and deliver different energies and organs exhibit different degree of radiosensitivity. Therefore, the concept of estimating internal dose should be developed by taking into account firstly the dynamic behaviour, e.g. retention and excretion, of the incorporated radionuclides in the body, i.e. aforementioned biokinetics.

The radionuclides deposited in different region will irradiate the organs and tissues around and themselves especially for alpha and beta emitters and this cross fire radiation fraction from source regions to target regions is defined as S values, now called S coefficients.[63] The determination of these S coefficients needs the spatial relation of anatomic organs and tissues, the human digital phantoms, and the radiation transport simulation with human phantoms applying Monte Carlo techniques. The organ absorbed dose can be then estimated by multiplying the activity in the source organ and the S coefficients from the source organ to the target organs under interest.

In the following, the human computational phantoms and the generalized formula recommended by ICRP and MIRD Committee are introduced. Furthermore the treatment of decay products in dose calculations and commonly used software in internal dosimetry are introduced.

1. Computational phantoms and Monte Carlo simulation

Mathematical phantoms were developed at Oak Ridge National Laboratory for MIRD Committee of the Society of Nuclear Medicine.[71] During the last three decades, a new type of anatomic phantom, so-called voxel phantoms were developed by various groups. Voxel phantoms are anatomic models of human body based on computed tomography, magnetic resonance or other medical images obtained from high-resolution scans of a single individual and provide a more realistic representation of human anatomy. These phantoms consist of a large number of volume elements (voxels). ICRP developed adult reference computational phantoms[72] in voxel format adapted voxel phantoms developed at Helmholtz Zentrum München, formerly GSF-National Research Center for Environment and Health to the organ mass and volume of ICRP reference person.[73]

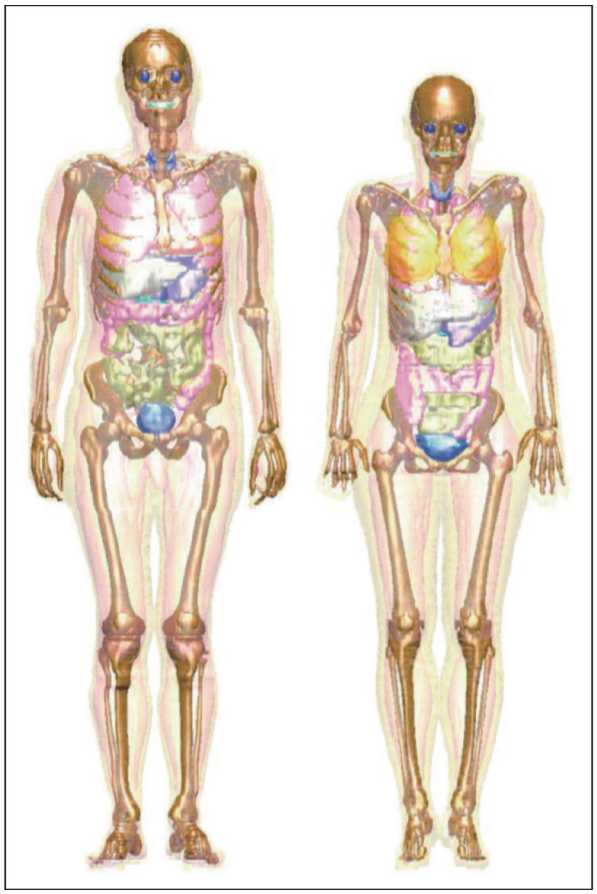

Fig. 11 Images of the adult male (left) and adult female (right) computational phantoms presented in ICRP Publication 110.[72] This picture is adopted from Fig. 3.1 of ICRP Publication 133 under the permission granted by ICRP on 27 January 2018.

Figure 11 shows images of the adult male (left) and adult female (right) computational voxel phantoms. The following organs can be identified by different surface colours: breast, bones, colon, eyes, lungs, liver, pancreas, small intestine, stomach, teeth, thyroid, and urinary bladder. Muscle and adipose tissue are semi-transparent.[72]

Calculations of the absorbed fractions (AFs) (see Appendix) for mono-energetic photons and electrons for the new reference computational phantoms were performed for the whole set of source regions listed in ICRP Publication 110.[72] For photons, energies from 10 keV to 10 MeV were considered and for electrons, energies between 15 keV and 10 MeV. For each energy, 5 million particle histories were followed through the body using the Monte Carlo transport code EGSnrc.[74] The specific absorbed fractions (SAFs) (Appendix) can further be calculated by dividing AFs by the mass in the target organ.

For photons it accounts for Rayleigh and bound Compton

scattering, pair production and photoelectric emission from *K*, *L* and *M* shells with subsequent emission of fluorescence or Auger/Coster-Kronig electrons. The cross sections agree with those of the XCOM/NIST database.[18]

Multiple electron scattering is performed with the electron collision stopping powers as recommended by ICRU[75] and the creation of bremsstrahlung is included. In particular, for electrons, the following calculations were performed: (1) AFs for both self-irradiation and cross-fire for solid soft-tissue organs. For cross-fire the anatomical position of a source or target region is more important than its size and shape; (2) AFs for cross-fire from solid soft-tissue organs to targets in the skeleton, in the HRTM, and in the HATM; (3) AFs for cross-fire from source regions in the skeleton (volume sources), in the HRTM, and in the HATM to solid soft-tissue organs; and (4) AFs for cross-fire between HRTM and HATM regions. It should be noted that the electron AFs of ICRP Publications 66[61] and 100[50] were used for those cases for which their values were neither 0 nor 1, i.e., those that were evaluated by other means than the simplifying assumptions of ICRP Publication 30.[37] For a complete calculation of AFs and SAFs values for other radiation types, e.g. recoil protons, alpha particles and neutrons and skeletal tissues, ICRP Publication on SAFs for reference adults can be referred.[76]

2. Generalized schema for internal dosimetry

ICRP developed a dosimetric schema focused on the occupational internal dosimetry for workers[37, 54–60, 77, 78] and members of the public.[38, 44, 45, 79, 80] The MIRD Committee focused only on medical internal radiation dose for patients.[81–83] However, ICRP developed as well dose coefficients for patients in diagnostic nuclear medicine.[84–87] In 2009, ICRP and MIRD generalized a standardized nomenclature for dosimetric models.[88] It is assumed that during a certain age period, the changes in anatomy for one age group will be neglected; in practical calculation, the time-independent formulation is used, and the dose-commitment period is standardized to 50 y for adults or a variable time to age 70 y for those exposed as infants, children, or adolescents. The mean absorbed dose coefficient was defined as Eq.(3):

$$d\,(r_T, T_D) = \sum_{r_S} \tilde{a}\,(r_T, T_D)\, S\,(r_T \leftarrow r_S) \tag{3}$$

where $S\,(r_T \leftarrow r_S) = \sum_i \dfrac{E_i\, Y_i\, \phi\,(r_T \leftarrow r_S, E_i)}{M(r_T)}$, this value is called SE (specific energy) in the previous dose calculation system (SEECAL),

where $\Phi\,(r_T \leftarrow r_S, E_i) = \dfrac{\phi\,(r_T \leftarrow r_S, E_i)}{M(r_T)}$, the specific absorbed fraction (SAF).

It is noted here that ϕ is age-dependent, so that Φ and S are age-dependent as well. To calculate the mean absorbed dose from childhood, the values at different age period will be quantified and summed up, so for equivalent dose and effective dose.

Equivalent dose coefficient can be calculated as Eq.(4):

$$h\,(r_T, T_D) = \sum_{r_s} \tilde{a}\,(r_s, T_D)\, S_w\,(r_T \leftarrow r_S) \tag{4}$$

where $S_w\,(r_T \leftarrow r_S) = \sum_R w_R \sum_i \dfrac{E_{R,i}\, Y_{R,i}\, \phi\,(r_T \leftarrow r_S, E_{R,i})}{M\,(r_T)}$.

This value is called SEE (specific effective energy) in the previous dose calculation system.[88, 89]

$h\,(r_T, T_D)$: Equivalent dose coefficient of organs r_T over the dose-integration period T_D.

$\tilde{a}\,(r_S, T_D)$: Time integrated activity coefficient;

$S_w\,(r_T \leftarrow r_S)$: Radiation-weighted *S*;

w_R: Radiation weighting factor;

$E_{R,i}$: Energy of radiation *i* of type *R* per nuclear transformation;

$Y_{R,i}$: Yield of radiation *i* of type *R* per nuclear transformation;

$\phi\,(r_T \leftarrow r_S, E_{R,i})$: Absorbed fraction: fraction of energy $E_{r,i}$ of radiation type *R* emitted within the source organ r_S that absorbed in the target organ r_T;

$M\,(r_T)$: Mass of the target tissue r_T.

Effective dose coefficient for adults is shown in Eq.(5):

$$e\,(\tau) = \sum_T w_T \left[\frac{h_T^M(\tau) + h_T^F(\tau)}{2}\right] \tag{5}$$

$h_T^M(\tau)$ and $h_T^F(\tau)$ are male and female equivalent dose; w_T is tissue weighting factor. Reference phantoms for children of various ages will be developed for use in the calculation of dose coefficients for members of the public.[19] At present, effective dose coefficient for infants, children, or adolescents can be calculated as: $e(\tau) = \Sigma_T w_T h_T(\tau)$, where $h_T(\tau)$ is equivalent dose in organ *T* for infants, children, or adolescents.

3. Treatment of decay products

Decay products behave independently as they are produced in the human body, for example, the biokinetic model of uranium and the biokinetic model of thorium as a progeny of uranium are different. Therefore, biokinetic models, the transfer rates and especially the model structures of different radionuclides are assumed to be independent in the biokinetic modelling. For a proper interconnection of biokinetic models with varying biokinetic model structures, two approaches have been proposed in ICRP Publication 71.[79]

In the first approach, biokinetics of a radionuclide in a chain is calculated by using its own biokinetic description. Thereafter, the non-existing compartments representing source regions receive a portion of nuclear transformations which are partitioned by mass fraction from the so-called “Other” tissue. This “Other” tissue represents all systemic tissues, which are not explicitly specified in a biokinetic model.

In the second approach, prior to biokinetic modelling, the biokinetic model of a radionuclide in a chain is expanded for the non-existing compartments and transfer rates so that all the biokinetic models of radionuclides in the chain comprise the same number of compartments and the same kinetic transfer pathways. The transfer rates of loss from these compartments are the same as the corresponding ‘Other’ compartments but the transfer rates to them are weighted by mass fractions of those of the corresponding ‘Other’ compartments. The

transfer rates to the 'Other' compartments should be reduced accordingly.

The treatment of decay products to dose are applied to systemic biokinetic models. Due to the lack of knowledge of the solubility and absorption of the daughter nuclides in human alimentary tract, without further information, it is assumed that the soluble phases of the decay products produced inside the human alimentary tract follow the same behaviours as their parent nuclides. This consideration may introduce a small uncertainty on ingestion dose coefficients. In the human respiratory tract, decay products are bound to aerosols and behave like the parent nuclides.

As an example, internal dose assessment of ^{232}Th by applying the new obtained biokinetic parameters used the first approach of independent biokinetic modelling.[90] In another work on dose assessment of ^{238}U by using the f_A factor obtained from experimental human biokinetic investigation,[91] the second approach was applied. The difference of the dose coefficients by applying the two different approaches is less than 5% when the masses of the unspecified source regions are small to the mass of "Other".[79] In the ICRP OIR series, the second approach is recommended to apply for treatment of decay products in biokinetic modelling.

4. Software for internal dosimetry

Internal radiation doses to tissues or organs can be calculated by following above introduced methods and procedures provided the intake activity, the intake pathway and radionuclides are known. However, the procedures can be programmed in a computer code and it speeds up the calculations, if the structures and parameters of biokinetic models and computational phantoms are default of the reference person. In some cases, structures and parameters of models may be requested to fit the new measured biokinetic data, or an individual phantom is needed for a personalized set of S coefficients, then a new dedicated computer program may be developed or available computer programs might be modified. In the following, several common used computer programs for biokinetic modelling and internal dose calculations are introduced.

SAAM II[92] is user friendly commercial software for compartmental modelling in general. It was initially developed in NIH for pharmacokinetic investigation and was later licenced to Washington University for further development and now is maintained by company. It was widely used in nuclear medicine for imaging based kinetic modelling and in biokinetic modelling in internal Dosimetry. SAAM II can be used in two modules: numerical and compartmental modules. It can be easily learned to setup models and fit models to measured data and estimate model parameters. If the accumulated activities in source organs are calculated by using this program, one can multiply the S or S_w coefficients (formerly SE or SEE values) calculated by another computer program SEECAL[89] and obtain the dose coefficients for interested radionuclides. The computer program SEECAL was developed at Oak Ridge National Lab (ORNL) and widely used for generating SEE values (now S_w coefficients) for many radionuclides based on the mathematical phantoms developed at ORNL as well.

DCAL[93] is free software for internal dosimetry calculation. It was as well developed at ORNL and used for generating dose coefficients according to the ICRP methodology. One can put parameters in the program to get dose coefficients in the main routes, such as inhalation, ingestion and injection. In DCAL, the biokinetic models and computational phantoms, exclusively ICRP reference models and phantoms, are predefined and cannot be changed. However, one can output a set of S coefficients for dose calculation by applying own developed or modified biokinetic models.

IMBA[94] is commercial software for professional internal dosimetry and monitoring program. It is developed at PHE, UK. IMBA is widely used for internal monitoring programme to estimate intake and personal dose based on monitoring data. However, solely adult ICRP biokinetic models and phantoms were implemented in the program. The program is dedicated for application in workplace and for occupational workers. One can change some parameters, like the f_A in HATM and aerosol size, clearance and absorption parameters in HRTM to obtain corresponding doses.

OLINDA/EXM[95] is commercial software for internal dose assessment in nuclear medicine. It was designed according to the MIRD methodology. It was received approval from the FDA and was distributed after 510(k) premarket notification. It is widely used by nuclear medicine department to practically estimate organ doses of patients or to provide dose report for new radiopharmaceuticals. Users can apply this program to fit the image-based dynamic activities and time-integrated activities in organs and select appropriate phantoms to calculate organ absorbed doses. User can also put available time-integrated activities in source organs to get the absorbed dose for patients.

Some other internal dose programs have been developed by organisations and individuals for specific use, among them: DOSAGE (D. Noβke, BfS code, private communication) and PLEIADES[96] for generation of ICRP dose coefficients; IDSS,[97] AIDE,[98] MONDAL[99] and IDEA system,[100] which implemented ICRP internal dose methodology and biokinetic models and reference S coefficients, for incorporation monitoring and internal dose assessment; IDAC[101] for estimation of patient doses from radiopharmaceuticals.

V UNCERTAINTY IN INTERNAL DOSIMETRY

Internal doses were estimated by using biokinetic models and computational human phantoms, which were built upon the basis of human physiology and anatomy. The model parameters are evaluated mostly on the basis of experimental data obtained from laboratory animals and humans. Because of the physiological variability of humans, the variations due to the extrapolation of animal data to humans, and the measurement techniques, the parameters showed a wide variation and uncertainty. The S coefficients calculated by using reference and individual computational phantoms, showed variability.

Therefore assessment of dose and health risk suffers a

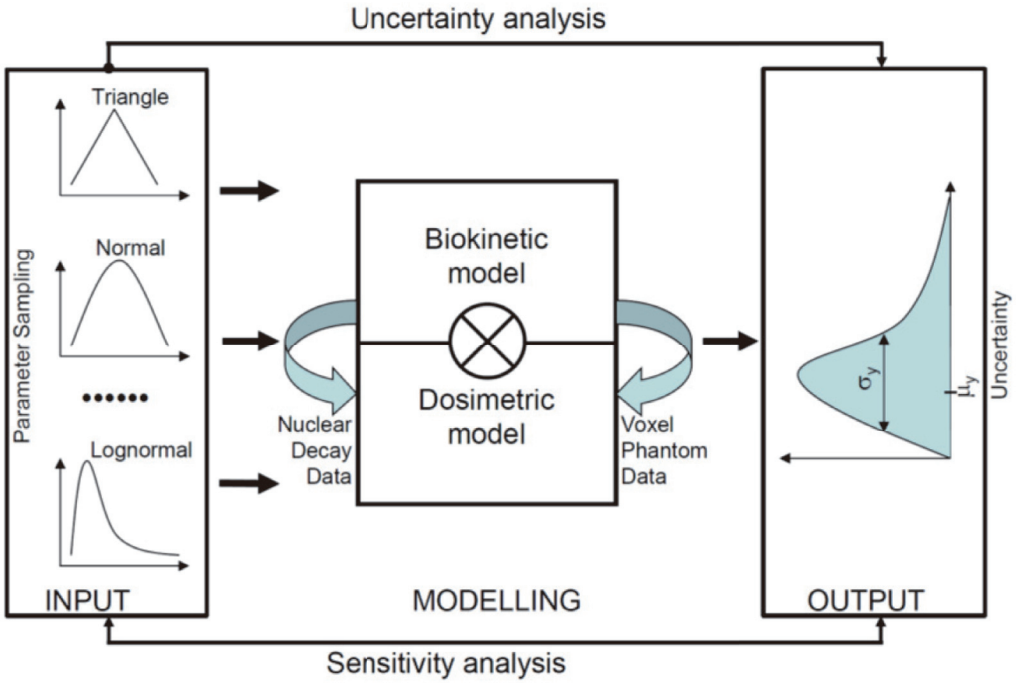

Fig. 12 Concept of uncertainty and sensitivity analysis in internal dosimetry.

large uncertainty and it needs a quantification of uncertainty. Furthermore, provided uncertainties can be identified, one can identify the most influential parameters in dose calculation procedures by applying sensitivity analysis method to guide further research effort in model calibration and even to reduce the dose uncertainty. Generally we apply the law of uncertainty propagation and Bayesian approach in the uncertainty and sensitivity analysis. **Figure 12** shows a general concept of uncertainty and sensitivity analysis in internal dosimetry

1. Uncertainty and sensitivity analysis

Uncertainties in data and models are origin for uncertainty analysis and sensitivity analysis. Uncertainty analysis is the computation of the total uncertainty induced in the output by quantified uncertainty in the inputs and models, and the attributes of the relative importance of the input uncertainties in terms of their contributions, whereas sensitivity analysis is the computation of the effect of changes in input values or assumptions, including boundaries and model functional form, on the outputs.[102] Generally the following steps were performed in the uncertainty analysis.

(1) Uncertainty of input: The sources of uncertainty of model parameters were carefully analysed and evaluated. Model structure is one uncertain factor. The ranges and distributions of model parameters were based on experimental measurement.

(2) Sampling: Sampling techniques are needed to generate samples of the model input parameters (variables). Generally, the random sampling technique, such as Monte Carlo simulation, or the stratified, such as the Latin hypercube sampling (LHS),[103] or quasi-random sequence sampling,[104] for example sampling based on Sobol sequence [105] are applied. Especially in sensitivity analysis, LHS and Sobol sequence sampling technique can improve the efficiency of Monte Carlo simulations by picking the input samples better and samples the entire domain more systematically.

(3) Modelling: To predict the kinetics and retentions of radionuclides or radiopharmaceuticals in humans, biokinetic modelling is required. One needs developing a computer program for biokinetic modelling and internal dose calculation. Hundreds to thousands of computer simulations should be performed with the sampled input parameters.

(4) Uncertainty of output: Model predictions for different organs and tissues at different time periods resulted in huge amounts of data. For a better presentation of this data, the percentile was used for data reduction and to interpret the uncertainty of the results. For each organ and tissue at a different time point, modelled data are presented as 2.5th, 50th and 97.5th percentiles for comprising the 95% confidence interval of the results.

Global sensitivity analysis (GSA) has recently been often used in contrast to local sensitivity analysis. GSA can further be classified into two main methods: sampling based regression methods and variance based methods. Bayesian sensitivity analysis can be classified into regression methods and can also be separately defined.

To identify the most influential parameter in a model, the concepts of the standardized rank regression coefficient (SRRC) and the partial rank correlation coefficient (PRCC) [106] were used. The SRRC can be computed by constructing regression models, which approximate the rank transformations of the sampled model input and output variables. The PRCC measures the rank correlation between one defined output variable with an input variable, under the

condition that the indirect influence on this defined output variable due to other further input variables is somehow eliminated.

Variance based method is increasingly, due to its generally model-free applicable, used in global sensitivity analysis.[107] The formula for absorbed dose calculation can be written as a function $Y = f(X_1, X_2, \ldots, X_k)$, where Y is the absorbed dose and X_i the parameters which represent the compartmental model and SAF values. For the ith parameter, the sensitivity indices S_i and S_{Ti} which measure for the first-order effect and the total effects can be written respectively as:

$$S_i = \frac{V_{X_i}[E_{X_{-i}}(Y|X_i)]}{V(Y)} \tag{6}$$

and

$$S_{Ti} = \frac{E_{X_{-i}}[V_{X_i}(Y|X_{-i})]}{V(Y)} \tag{7}$$

where $V(Y)$ is the unconditional variance of Y; $V_{X_i}[E_{X_{-i}}(Y|X_i)]$ is the expected reduction in variance of Y if X_i is fixed; $E_{X_{-i}}(Y|X_i)$ is the mean of Y taken over all parameters but X_i; $E_{X_{-i}}[V_{Xi}(Y|X_{-i})]$ is the expected variance that is left if all parameters but X_i is fixed; $V_{Xi}(Y|X_{-i})$ is the variance of Y taken over X_i.

The sensitivity indices S_i and S_{Ti} for each ith parameter can be calculated by Eq.(6) and Eq.(7). If the biokinetic parameters are classified to $b1$ to bn, and the cross-fire SAF values are classified to $p1$ to pn, then the sensitivity indices S_{bi}, S_{pi} and S_{Tbi}, S_{Tpi} for each parameter b_i and p_i can be calculated with the best available practical estimator:[107, 108]

$$V(Y) = \frac{1}{N}\sum_{j=1}^{N} f(\boldsymbol{A})_j f(\boldsymbol{B})_j -$$

$$\left[\frac{1}{N}\sum_{j=1}^{N} f(\boldsymbol{A})_j\right]\left[\frac{1}{N}\sum_{j=1}^{N} f(\boldsymbol{B})_j\right] \tag{8}$$

$$V_{Xi}[E_{X-i}(Y|X_i)] = \frac{1}{N}\sum_{j=1}^{N} f(\boldsymbol{B})_j [f(\boldsymbol{A}_{\boldsymbol{B}}^{(i)})_j - f(\boldsymbol{A})_j] \tag{9}$$

$$E_{X-i}[V_{Xi}(Y|X_{X-i})] = \frac{1}{2N}\sum_{j=1}^{N} [f(\boldsymbol{A})_j - f(\boldsymbol{A}_{\boldsymbol{B}}^{(i)})_j]^2 \tag{10}$$

where $\boldsymbol{A}$ and $\boldsymbol{B}$ are independently generated sample matrices, each consists of N samples of all the parameters; $\boldsymbol{A}_{\boldsymbol{B}}^{(i)}$ is a sample matrix formed by all columns of $\boldsymbol{A}$ except ith column, which is taken from $\boldsymbol{B}$. Here the column index i is defined as for columns which represents the biokinetic model parameter (bi) or the cross-fire SAF value (pi). This global variance based sensitivity analysis method was applied to the uncertainty budget from biokinetic model parameters and voxel phantoms to internal dose of patients received from radiopharmaceuticals.[109]

2. Bayesian model uncertainty analysis

Reference or standard biokinetic models are developed and reported by ICRP based on up-to-date human and animal data. In some cases, for example, individual monitoring or specific patient dose assessment, new personalized biokinetic data are obtained, models other than ICRP reference models are build up for specific applications. In this context, the structures of the biokinetic modes, in addition to uncertainty of parameters, can contribute to the uncertainty of dose assessment and monitoring. Methods developed in the framework of Bayesian statistics can be used by taking into account the uncertainties from different model structures and parameters simultaneously,[110] furthermore, provided several models are equally fit the measured data, Bayesian model selection[111] and Bayesian model averaging[112] can be applied to select an optimal model or jointly adopt different model structures and parameters for practical use, respectively.

Bayesian model selection can be performed in the following steps: (1) Formulation of biokinetic models in a system of differential equations, Eq.(11); (2) Availability of measured data, for example, in blood and urine or organ contents, Eq.(12); (3) Evaluation of the prior distributions, Eq.(13); (4) Building the likelihood function and calculating the marginal density, Eq.(14); (5) Calculation of the posterior probability by applying the Bayes theorem, Eq.(15); (6) Calculation of Bayes factor, Eq.(16) and selecting a model.

$$dy_j^k(t)/dt = \sum x_{+j}^k y_j^k(t) - \sum x_{-j}^k y_j^k(t) \tag{11}$$

where: x_{+j} is the set of indices of all transfer rates flowing into compartment y_j; x_{-j} the set of indices of all transfer rates flowing out of compartment y_j; k indicates different models.

$$D_i = (y_b^{i,1}, y_b^{i,2}, \ldots, y_b^{i,n_i^b}, y_u^{i,1}, y_u^{i,2}, \ldots, y_u^{i,n_i^u}) \tag{12}$$

Where: D_i is the data set and n_i^b and n_i^u the number of measurement in blood y_b and in urine y_u for subject i.

The multivariate prior distribution $p(\mathbf{x}_k|k)$ of model k was taken to be the product of the univariate prior distributions $p(x_k^r|k)$ for each parameter x_k^r:

$$p(\mathbf{x}_k|k) = \Pi_r p(x_k^r|k) \tag{13}$$

The marginal density $p(D_i|k)$ (also called data evidence) can be obtained by integrating the product of likelihood function and the prior distribution over the according parameter space $\boldsymbol{X}_k$, and it is the basis for the model selection process.

$$p(D_i|k) = \int_{Xk} L_i(x_k, k|D_i)\, p(x_k|k)\, dx_k \tag{14}$$

where: $L_i(x_k, k|D_i)$ is the likelihood function.

The posterior probability for choosing model k or k' against data can be calculated by Eq.(15):

$$p(k|D_i) = \frac{p(D_i|k)\,p(k)}{p(D_i)}, \; p(k'|D_i) = \frac{p(D_i|k')\,p(k')}{p(D_i)} \tag{15}$$

Bayes factor can be calculated by Eq.(16), most importantly, a Bayes factor $B_{k,k'}^i > 3$ substantially favors model k, while $B_{k,k'}^i > 100$ decisively favors model k.

$$B_{k,k'}^i = \frac{p(D_i|k)}{p(D_i|k')} \tag{16}$$

The above mentioned method was successfully applied to select a best model from the HMGU and ICRP biokinetic models of strontium (**Fig. 13**) based on the measured human data.[113]

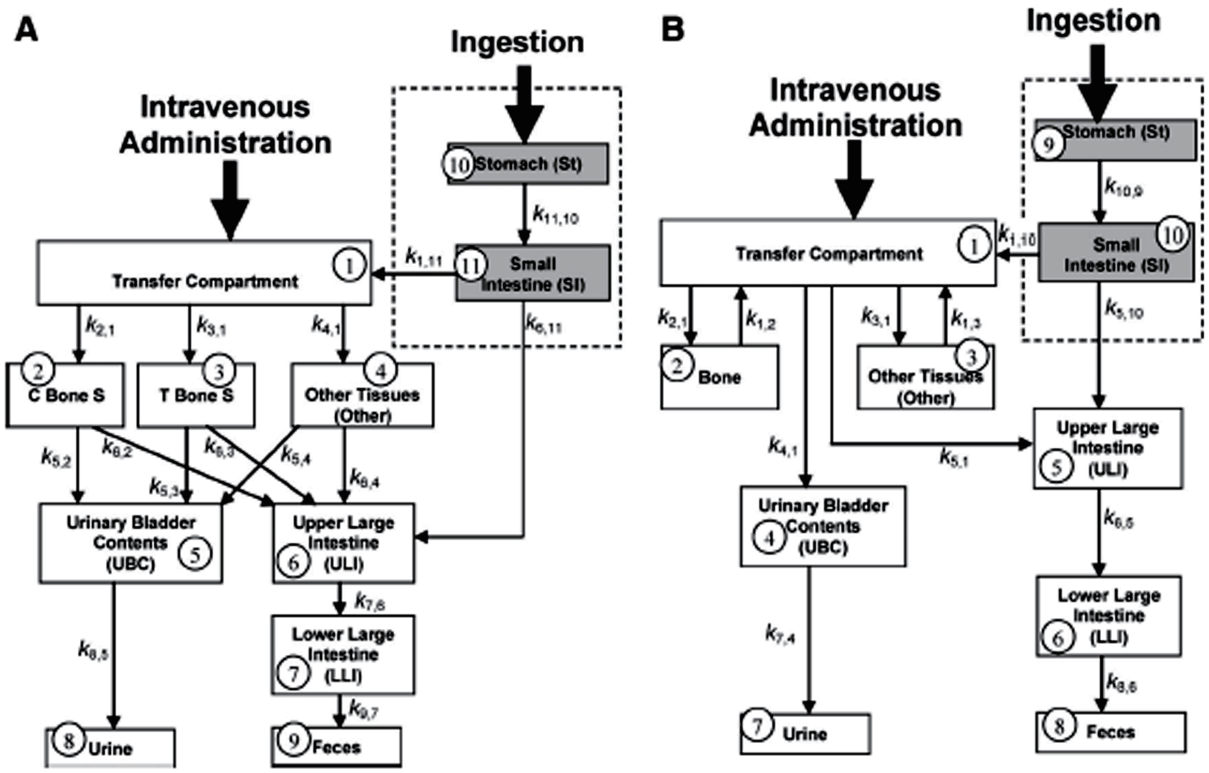

Fig. 13 ICRP (A) and HMGU (B) zirconium biokinetic compartmental models.[113] Transfer compartment — blood; C Bone S — Cortical bone surfaces; T Bone S — trabecular bone surfaces.

Based on results of Bayesian model selection, Bayesian model averaging can be performed as Eq.(17) by taking into account different models, M_k and their parameters, θ_k considered:

$$p(x|D) = \sum_{k=1}^{K} p(x|M_k, D)\, p(M_k|D) \tag{17}$$

where:

$$p(M_k|D) = \frac{p(D|M_k)\, p(M_k)}{\sum_{l=1}^{K} p(D|M_l)\, p(M_l)}$$

$$p(D|M_k) = \int_{M_k} p(D|\theta_k, M_k)\, p(\theta_k|M_k)\, d\theta_k$$

VI APPLICATIONS

1. Radiation protection

In radiation protection, the internal dose coefficients of incorporated radionuclides are needed to assess the health risk of the workers and members of the public. These dose coefficients were calculated according to the newly revised biokinetic models and the voxel phantoms and were implemented by national and international Basic Safety Standards (BSS)[114] and EU Directive 2013/59/EURATOM.[115] In the following, the calculation of age-dependent inhalation dose coefficients for ^{238}U for members of the public is shown.

First, the inhalation physiological parameters and age-dependent biokinetic models (**Fig. 9**) for the six defined age groups (infant, 1-y, 5-y children, 10-y young child and 15-y and adults) were used to calculate the inhalation input and the time integrated activity (A), up to age 70 years and 50 years for children and adult, respectively.

To calculate the A, one should be able to solve the age-dependent biokinetic models. There are several ways to solve the first-order differential equations by using available software, SAAM II or MATLAB etc., or using available codes or write own program to solve the problem. In the biokinetic modelling, the age-dependent parameters were linear interpolated. The decay products were treated by the methods recommended by the ICRP.[63] Three daughters of the ^{238}U are needed to be calculated because the contributions of the other daughters to organ doses can be neglected. To check till which decay products the biokinetic models are needed, one can refer to ICRP Publication 30 series or using the software WinChain.[116] After solving the complex differential equations, the retention curves in each organ can be integrated up to age 70 years or over 50 years.

For reference person, ICRP provides reference voxel computational phantoms[72] and the SEE values (now S_w coefficients) are usually provided in document, for example in ICRP Publication 30 series[37] with mathematical phantoms and ICRP Publication 133[76] based voxel phantoms, or provided by application software, SEECAL.[89] In the future, the SEECAL may be updated with the reference voxel phantoms and users can use it for calculating the S_w coefficients of different radionuclides. For individual dose assessment, one should select a phantom from available phantom library whose anatomic data is close to the person under investigation. In this

example, the age-dependent S_w coefficients were calculated by SEECAL with the mathematical phantoms.

Applying the dosimetric formula, one can obtain the inhalation equivalent dose coefficients first and by multiplying the tissue weighting factors w_T; the effective dose can be calculated. These estimated dose coefficients can be used to make decisions if some measures should be taken for protection of people from radiation.[66, 117)]

2. Internal exposure monitoring

In order to protect workers, in Europe workplace monitoring is required for controlling the limit on the effective dose for occupational exposure:[115)] 20 mSv in any single year or up to 50 mSv in special circumstances or for certain exposure situations specified in national legislation. In contamination accident, internal monitoring program is used to assess possible intake and internal doses for risk or biological effects assessment. For a dose assessment of internal monitoring, the whole body retention or organ retention, in some cases, the daily urinary or faecal excretion is needed. Applying the biokinetic models to measured data and the appropriate monitoring programs are well descripted and documented in ICRP Publication 78. Here we present a real ^{226}Ra contamination case[118)] by using partial body monitoring and related biokinetic model to assess the internal organ dose and the risk to a specific person (denoted as Mr. J).

Mr. J was working as a radar soldier in Germany for many years and was diagnosed colon cancer in 2003 and dead in May 2007. His relative complained that the cancer was attributed by ^{226}Ra contamination during his working time from 1977 to the end of 1985. He was monitored at HMGU by partial body counters on the skull in March 2007. To assert the mortality risk of contamination of ^{226}Ra during his occupational activity, the possible incorporation of ^{226}Ra and the colon dose assessment are requested by the Unfallkasse des Bundes (federal accident insurance) in Germany.

The age-dependent biokinetic model of radium was implemented for the early times before Mr. J participated in work and the routes of incorporation were combined by ingestion and inhalations. The consumption of ^{226}Ra by ingestion from food and drinking water and inhalation out of working time is assumed to be the average value in the Germany. The inhalation and ingestion rate during the working time of Mr. J was retrospectively calculated by using the age-dependent model fitting to measured activity in skull bone. The colon dose and effective dose to Mr. J by inhalation and ingestion can then be estimated, respectively. The mortality risk can be assessed by using the risk table of ^{226}Ra, so that the regulator can decide if a refund should be reimbursed to the Mr. J.

Figure 14 shows the biokinetic models for ingestion and inhalation of Ra, they are coupling of the systemic model of Ra and GIT model and HRTM. The intake of Ra by Mr. J out of working time is estimated and listed in **Table 2**. The fitted retention curves in bone by ingestion and inhalation are shown in **Fig. 15**. The equivalent dose in bone and effective doses are presented in **Table 3**.

Based skull bone measurement, applying biokinetic modelling and internal dosimetry, it is retrospectively estimated that Mr. J. possibly received an equivalent dose to colon, up to 6.2 mSv and an effective dose, up to 0.25 Sv, which are much higher than the natural exposure, say, 0.3 mS for colon and 1.3 mSv as effective dose.

Biokinetic and dosimetric models were used to retrospectively estimate the possible intake of radionuclide ^{210}Po for the ex-Russian spy Alexander Litvinenko.[119)]

3. Radon and its progeny

Radon and its progeny are responsible for more than 50% of annual effective doses to members of the public worldwide.[120)] We show here an example[121)] how the inhalation doses to different groups of members of the public are calculated according to the ICRP biokinetic and dosimetric models.[122)]

(1) Physiological parameters and depositions

The deposition fractions of radon progeny attached to aerosol particles in the human respiratory tract depend on aerosol particle sizes and physiological parameters like age, sex and life style. To cover the particle sizes of radon progeny in indoor air, deposition fractions of four aerosol sizes in activity median aerodynamic diameters (AMAD) and activity median thermodynamic diameter (AMTD): 50 nm, 230 nm and 2,500 nm for attached aerosols and 1 nm representing the unattached progeny were calculated by a logarithmic interpolation of the published deposition fraction values in the ICRP Publication 66 by using a six-term exponential function. The typical indoor time budget distribution of different activities for the human being is supposed as 71% and 29% for sleeping and light exercise respectively for three month infant and 55%, 15%, and 30% for sleeping, sitting, and light exercise, respectively for all other age groups.

(2) Biokinetic models

A general compartmental model **(Fig. 16**) was constructed by coupling the systemic models of the radon progeny, HRTM[61)] and GIT model[37)] to model the biokinetics of inhaled radionuclides in human lungs and retention in other organs and tissues. The systemic models for different progeny are independent; the structures and parameters of biokinetic models for different progeny are therefore different. In biokinetic modelling, age-dependent transfer rates and the treatment of decay products of radon progeny are implemented. For treatment of decay progeny generated in the human body, the first approach suggested by ICRP in Publication 71[79)] (see section IV.3) was applied.

The complete dynamic transfer process of the inhaled radon progeny in the lungs and between the organs can be described by a system of first-order linear differential equations and can be solved by using software SAAM II[92)] (The Epsilon Group VA, USA). The time-integrated activity, $\tilde{A}$ from any radon progeny in each organ was calculated by integrating the radioactivity in the organ up to the age of 70 years for children and over the 50 years commitment period for adults following the intake.

(3) Equivalent dose and effective dose

Equivalent doses were calculated with time-integrated

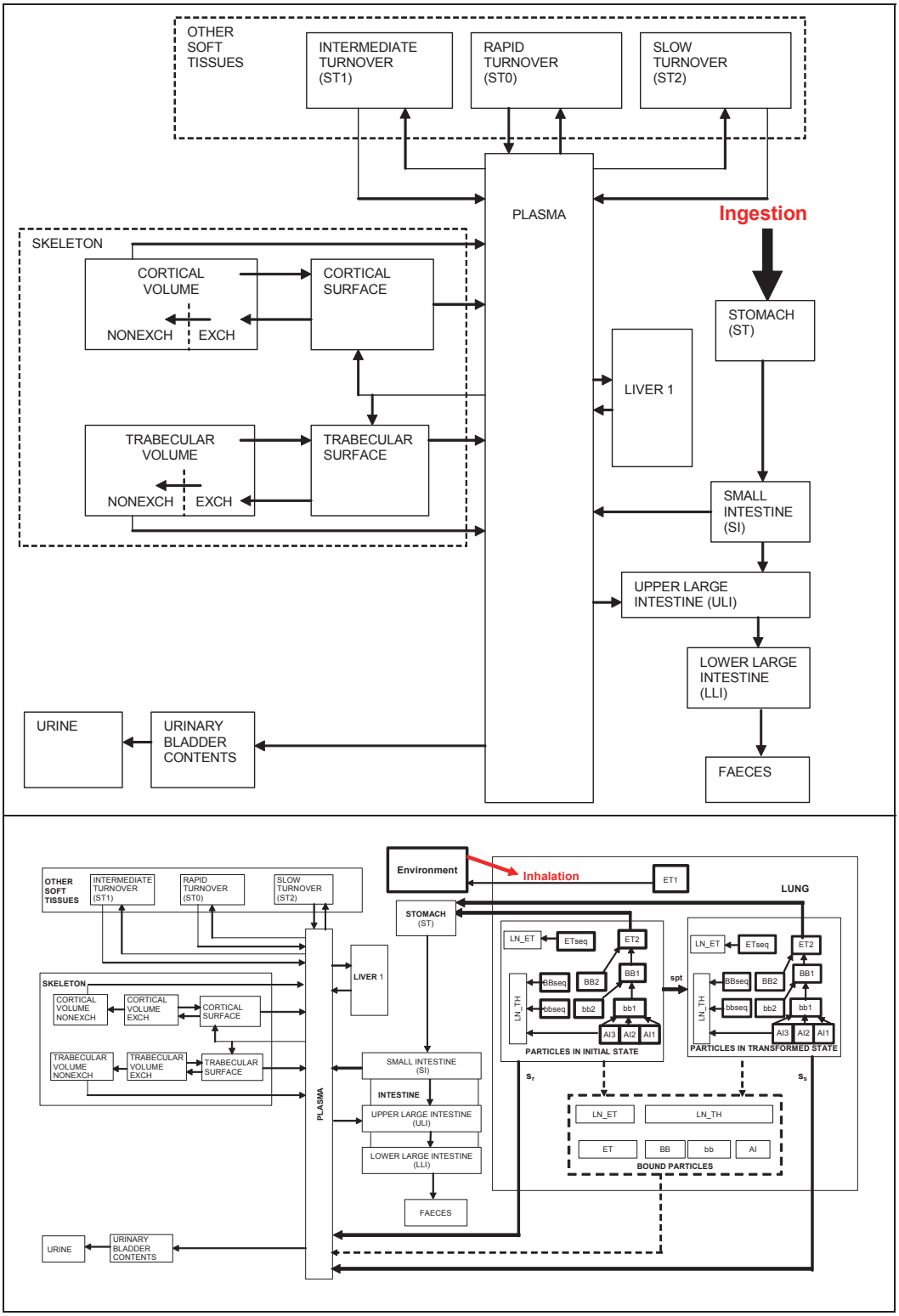

Fig. 14 Age-dependent biokinetic models of Ra for ingestion (upper) and inhalation (lower) based on the systemic biokinetic model of Ra and GIT model and HRTM.

Table 2 Estimated intake of Ra by Mr. J during his life, t_1, t_2 are the beginning and end time of work employment, t_3 and t_M are diagnostic time and time of death, respectively.

Mr. J						t_1(J)	t_2(J)	t_3(J)	t_M
Time (d)	90	365	1,825	3,650	5,475	8,891	11,843	18,128	19,586
Ingestion (Bq d^{-1})	3.3×10^{-2}	5.5×10^{-2}	7.1×10^{-2}	8.5×10^{-2}	9.6×10^{-2}	1.1×10^{-1}	**20.0**	1.1×10^{-1}	1.1×10^{-1}
Inhalation (Bq d^{-1})	6.8×10^{-6}	1.2×10^{-5}	2.0×10^{-5}	3.5×10^{-5}	4.5×10^{-5}	5.0×10^{-5}	**38.3**	5.0×10^{-5}	5.0×10^{-5}

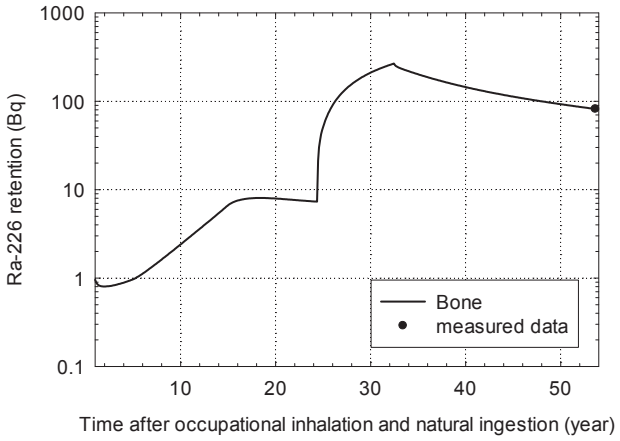

Fig. 15 Model prediction of retention of ^{226}Ra after a protracted inhalation until the monitoring time based on the measured activity in bone for a possible contamination case of ^{226}Ra.

activity and the radiation-weighted S_W coefficients. Effective dose, E, for 15 year olds and adults, are calculated by averaging the effective doses of female and male according to Eq.(5). For other age groups, effective doses were calculated following ICRP 1990 Recommendations[24] without taking into account the difference between females and males.

(4) Dose conversion factor

The effective dose of inhaled short-lived radon progeny is expressed normally in dose conversion factor and is calculated by suggestion in ICRP Publication 130[63] in Eq.(18) as effective dose per unit potential alpha energy exposure in unit of Sv per J h m^{-3} or in unit of Sv per WLM (1 WLM = 3.54×10^{-3} J h m^{-3}. One WLM equals about 6.37×10^5 Bq h m^{-3} of equilibrium equivalent concentration (EEC) of ^{222}Rn):

$$E(Sv\ per\ WLM) = \sum_{i=1}^{4} \sum_{j=1}^{4} C_{j,i} B\, t\, f_{pj} E_{j,i} \qquad (18)$$

The index i corresponds to inhaled radon progeny; $i = 1$, 2, 3 and 4, for ^{218}Po, ^{214}Pb, ^{214}Bi and ^{214}Po respectively. Index j corresponds to the aerosol mode of the activity size distribution; $j = 1$, 2, 3 and 4 for the unattached, nucleation, accumulation and coarse modes respectively. The symbol $C_{j,i}$ is the activity concentration of the decay product i and activity size distribution j corresponding to a radon progeny mixture of 1 WL, B is the average breathing rate for each age group, t is taken as the exposure period of 170 h, f_{pj} is fraction of the potential alpha energy concentration (PAEC) associated with mode j and $E_{j,i}$ is the effective dose coefficient for decay product i with an activity size distribution for mode j.

Similar calculation procedure for thoron progeny can be referred to Bi et al.[123] The study on comparison of skin dose and inhalation is recently studied by Sakoda et al.[69] The calculated dose conversion factors for radon and thoron progeny are practically used to assess the annual dose contributions for dwellings with earthen architecture in Germany.[124] For example in one house, it is shown the annual dose of 1 to 2 mSv from radon progeny in the upper floor and 3 to 6 mSv in the ground floor and additional 1 to 2 mSv from thoron progeny with slightly smaller values in the adjacent rooms without thoron-exhaling building material. In another house about 1 to 5 mSv from radon progeny and 1 to 2 mSv from thoron progeny were calculated for the living room under usual living conditions and 12 and 9 mSv, respectively, for the guestroom under the condition of low ventilation. These annual doses provide essential dose information for risk assessment for the people who are living there.

4. Nuclear medicine imaging and radiotherapy

We introduced here one example of using biokinetic modelling and dosimetric method on dose assessment of patients to ^{18}F-FDG in diagnostic nuclear medicine.[125] ^{18}F-FDG is a mostly used radiopharmaceutical in nuclear medicine for detecting cancers. A compartmental model[126] for ^{18}F-FDG was developed by MIRD Committee based on five adult human volunteers. The model (**Fig. 17**) was in principle set up with each of the measured organs represented by a single compartment in exchange with the plasma, plus (in the case of the myocardium, lungs and liver) and adjustable fraction of the plasma and erythrocyte compartments. The parameters for FDG in brain kinetics[127] were incorporated into this model. Model parameters were estimated by implementing the compartmental model and the measured data in a previous version of software SAAM II. **Table 4** showed estimated model parameters. The dynamic blood kinetics is important for building up biokinetic models of many radiopharmaceuticals. There are several methods to determine the blood concentration, e.g. images, blood sampling, in vivo measurement.[128] If the blood data is lack, the reference tissues compartmental model can be applied.[129, 130]

In calculating the organ doses, a dynamic kidney model[49] was used. The advantage of this dynamic model is that the voiding time can be taken into account and the dose to bladder wall can be more precisely estimated. The organ absorbed dose was calculated by using the software OLINDA/EXM.[95] In clinical practice, activities in organs were estimated from images at different times, the dynamic image-based organ activities can be fitted by exponential functions without applying compartmental modelling and the time-integrated

Table 3 Estimated organ doses and effective dose for Mr. J based on natural intake of ^{226}Ra, and dose limit estimated based on the potential additional occupational intake of ^{226}Ra in Table 2 (20.0 Bq per day by ingestion and 38.3 Bq per day by inhalation).

	Natural ^{226}Ra		Additional ^{226}Ra during work	
Organ	Ingestion	Inhalation	Ingestion	Inhalation
Respiratory Tract	(Sv Bq^{-1})	(Sv Bq^{-1})	(Sv Bq^{-1})	(Sv Bq^{-1})
ET Airways	1.1×10^{-4}	5.6×10^{-6}	2.3×10^{-3}	1.5
Lungs	1.1×10^{-4}	2.6×10^{-5}	2.3×10^{-3}	1.9
Bladder Wall	1.1×10^{-4}	2.2×10^{-8}	2.3×10^{-3}	3.2×10^{-3}
Breast	1.1×10^{-4}	2.2×10^{-8}	2.3×10^{-3}	3.2×10^{-3}
Brain	1.2×10^{-4}	2.2×10^{-8}	2.4×10^{-3}	3.2×10^{-3}
Skin	1.1×10^{-4}	2.2×10^{-8}	2.3×10^{-3}	3.2×10^{-3}
Testes	1.2×10^{-4}	2.3×10^{-8}	2.3×10^{-3}	3.2×10^{-3}
Bone Surfaces	7.3×10^{-2}	1.4×10^{-5}	7.0×10^{-1}	9.4×10^{-1}
Liver	6.0×10^{-4}	1.1×10^{-7}	1.1×10^{-2}	1.4×10^{-2}
GI Tract				
Oesophagus	1.1×10^{-4}	2.2×10^{-8}	2.3×10^{-3}	3.2×10^{-3}
Stomach Wall	1.2×10^{-4}	2.2×10^{-8}	2.4×10^{-3}	3.2×10^{-3}
Small Intestine	1.2×10^{-4}	2.2×10^{-8}	2.5×10^{-3}	3.3×10^{-3}
ULI Wall	1.7×10^{-4}	3.0×10^{-8}	3.8×10^{-3}	4.5×10^{-3}
LLI Wall	3.9×10^{-4}	5.9×10^{-8}	8.8×10^{-3}	8.7×10^{-3}
Colon	2.7×10^{-4}	4.3×10^{-8}	5.8×10^{-3}	6.2×10^{-3}
Spleen	2.1×10^{-4}	3.8×10^{-8}	3.1×10^{-3}	4.2×10^{-3}
Muscle	1.1×10^{-4}	2.2×10^{-8}	2.3×10^{-3}	3.2×10^{-3}
Adrenals	1.2×10^{-4}	2.2×10^{-8}	2.4×10^{-3}	3.3×10^{-3}
Kidneys	2.4×10^{-4}	4.4×10^{-8}	3.5×10^{-3}	4.6×10^{-3}
Ovaries	1.2×10^{-4}	2.2×10^{-8}	2.4×10^{-3}	3.2×10^{-3}
Pancreas	1.1×10^{-4}	2.2×10^{-8}	2.3×10^{-3}	3.2×10^{-3}
Red Marrow	3.8×10^{-3}	7.0×10^{-7}	5.1×10^{-2}	6.9×10^{-2}
Thyroid	1.1×10^{-4}	2.2×10^{-8}	2.3×10^{-3}	3.2×10^{-3}
Thymus	1.1×10^{-4}	2.2×10^{-8}	2.3×10^{-3}	3.2×10^{-3}
Uterus	1.1×10^{-4}	2.2×10^{-8}	2.3×10^{-3}	3.2×10^{-3}
Effective dose	1.3×10^{-3}	3.3×10^{-6}	1.6×10^{-2}	2.5×10^{-1}

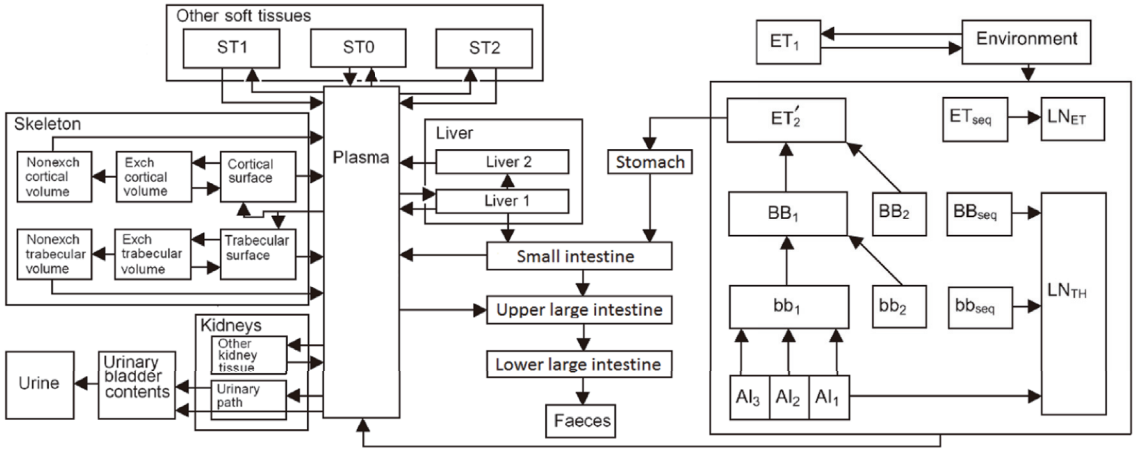

Fig. 16 Biokinetic compartmental model for inhalation of radon progeny.[121]

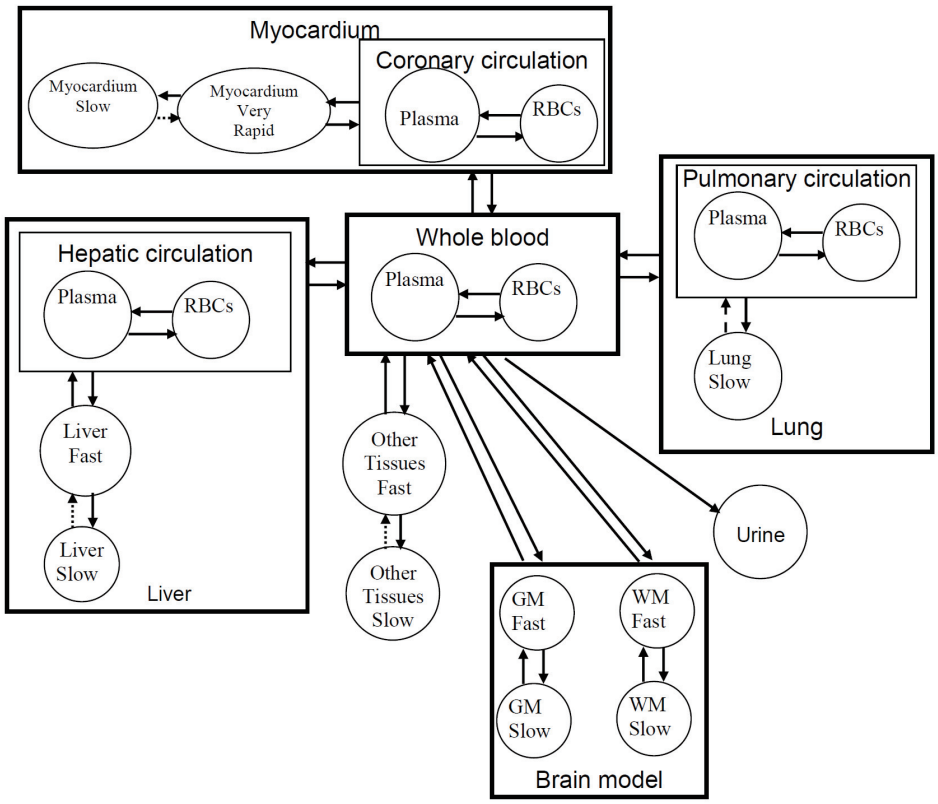

Fig. 17 A compartmental model for ^{18}F-FDG used for dose estimation by MIRD Committee.[125] (The figure was reproduced after the Figure 1 in reference.)[126]

Table 4 Parameters estimated by fitting the compartmental model to the PET images and urinary excretion (n = 10).

	Combined data from glucose and fasting sessions (min^{-1})		
Parameter	Mean	SD*	Geometric mean
Whole-body parameters			
Plasma to erythrocytes	4.80	2.92	4.07
Erythrocytes to plasma	8.07	2.85	7.35
Plasma to fast "other"	0.371	0.127	0.348
Fast "other" to plasma	0.102	0.034	0.097
Fast "other" to slow "other"	0.0167	0.0073	0.015
Plasma to urine	0.0088	0.0022	0.0085
Myocardial parameters			
Plasma to myocardium	0.0053	0.0044	0.003
Fraction of blood volume "seen"**	0.069	0.011	0.068
Lung parameters			
Plasma to Lung	0.0017	0.0006	0.0016
Fraction of blood volume in lung	0.15	0.036	0.148
Liver parameters			
Plasma to fast liver	0.068	0.069	0.038
Fast liver to plasma	0.219	0.108	0.186
Fast liver to liver "sink"	0.018	0.023	0.006
Fraction of blood volume in liver	0.243	0.172	0.202

* SD - Standard deviation.

** About 2% of blood volume is estimated for coronary artery content. Balance represents the "very rapid" myocardial exchange pool.

Table shows fraction of donor compartment transferred to recipient compartment each minute.

activities can be further calculated by area under the curve. This function is available in software OLINDA/EXM. The calculated absorbed doses to patients are important dose information for further risk estimation of secondary cancer or control of dose limits for patients for further treatment.

VII SUMMARY AND FURTURE OF INTERNAL DOSIMTRY

This review attempts to give a short and concise orientation on the methodology and techniques used in the internal dosimetry and several essential applications. The concept of internal dosimetry developed by ICRP was highlighted here and the development of MIRD Committee on patient doses to radiopharmaceuticals was taken as complementary to that of ICRP. The basic physical interactions between radiation and matters, especially for liquid water and DNA moieties were briefly introduced, the chemical and biological effects of radiation on humans and the consequential health risk are briefly explored. Then the biokinetic models of incorporated radionuclide for diverse routes were descripted. The dosimetric models developed by ICRP system and the computational phantoms and Monte Carlo simulation technique were shortly introduced. The treatment of decay products and uncertainty analysis in internal dose calculations were highlighted as well. At last, applications of internal dosimetry and several calculations were given as examples. In addition, the elemental dosimetric quantities used in internal dosimetry and biokinetic models in ICRP publications were given in the appendix.

Although the ICRP and MIRD Committee reach a consensus on the nomenclature on the dosimetric quantities, ICRP is continually focusing on radiation protection of internal exposures for occupational workers and member of the public including medical exposure; MIRD is focusing only on radiation doses to patients in diagnostic and therapeutic nuclear medicine. In the near future, after finalizing the OIR series on the biokinetic models and dose coefficients of the occupational intake of radionuclides, the age-dependent computational phantoms for member of the public will be carried out and the new publication series on the next generation of age-dependent biokinetic models and dose coefficients for members of the public may take for some years.

The development of mesh-type reference computational phantoms for adults and children will be the next task in improvement of computational phantoms; so that the age-dependent reference computational voxel phantoms might be transferred to mesh-type phantoms.

Implementation of the next-generation biokinetic models and dose coefficients in exposure monitoring and in the national and international regulation and authorities could generate cooperative projects in the national and international levels.

In the framework of MIRD Committee, biokinetic models and dose coefficients for new radiopharmaceuticals will be constantly reported and the focus on paediatric dose optimisation will be strengthened.[131] As new radiopharmaceuticals with β- and α-emitters are approved in the clinical practise, the need of internal dose assessment to patients in the cellular level may stimulate the application of internal microdosimetry[132] in targeted radionuclide therapy and this development might motivate biokinetic modelling in microscopic levels.

ACKNOWLEDGEMENTS

Author thanks Dr. Akihiro Sakoda, Dr. Dietmar Noßke and Dr. Jochen Tschiersch for proof reading and scientific suggestions on the review.

REFERENCES

1) K. F. Eckerman, N. Ishigure, A. Phipps and J. W. Stather; Internal dosimetry of radionuclides. In: eds A. Kaul and D. Becker Radiological Protection (Landolt-Börnstein: Numerical Data and Functional Relationships in Science and Technology-New Series) Vol. VIII/4 (2005), Springer, Berlin.
2) G. J. Hine and G. L. Brownell; Radiation dosimetry (1956), Academic Press Inc., New York.
3) O. G. Raabe; Introdcution to internal radiation dosimetry. In: O.G. Raab ed., Internal radiation dosimetry (1994), Medical Physics Publishing, Madison, Wisconsin.
4) C. A. Potter; Internal dosimetry: a review. *Health Phys.*, **88**, 565−578 (2005).
5) M. Berman; MIRD Pamphlet No. 12: Kinetic models for absorbed dose calculations, p. 1−14 (1976).
6) H. D. Roedler; Biokinetik radioaktiver Stoffe (1986), Urban & Schwarzenberg, München Wien Baltimore.
7) R. L. Kathren and R. K. Burklin; Acute chemical toxicity of uranium. *Health Phys.*, **94**, 170−179 (2008).
8) W. Jacobi; The concept of the effective dose; a proposal for the combination of organ doses. *Radiat. Environ. Biophys.*, **12**, 101−109 (1975).
9) D. E. Lea; Actions of radiations on living cells. 2nd. Edition. Reprinted (1956), Cambridge: Cambridge University Press, UK.
10) W. C. Roesch; Microdosimetry of internal sources. *Radiat. Res.*, **70**, 494−510 (1977).
11) W. B. Li, W. Friedland, E. Pomplun, P. Jacob, H. G. Paretzke, M. Lassmann and C. Reiners; Track structures and dose distributions from decays of ^{131}I and ^{125}I in and around water spheres simulating micrometastases of differentiated thyroid cancer. *Radiat. Res.*, **156**, 419−429 (2001).
12) W. Z. Xie, W. Friedland, W. B. Li, C. Y. Li, U. Oeh, R. Qiu, J. L. Li and C. Hoeschen; Simulation on the molecular radiosensitization effect of gold nanoparticles in cells irradiated by x-rays. *Phys. Med. Biol.*, **60**, 6195−6212 (2015).
13) ICRU; Fundamental quantities and units for ionizing radiation (Revised). ICRU Report No. 85 (2011).
14) M. Dingfelder, D. Hantke, M. Inokuti and H. G. Paretzke; Electron inelastic-scattering cross sections in liquid water. *Radiat. Phys. Chem.*, **53**, 1−18 (1999).
15) P. Bernhardt and H. G. Paretzke; Calculation of electron impact ionization cross sections of DNA using the

Deutsch-Märk and Binary-Encounter-Bethe formalisms. *Int. J. Mass Spectrometry*, 223−224, 599−611 (2003).
16) H. G. Paretzke; Radiation track structure theory. In: G. R. Freeman ed. Kinetics of nonhomogeneous processes. pp 89−170 (1987), John Wiley & Sons, New York.
17) R. D. Evans; The atomic nucleus (1955), McGraw-Hill Book Company, New York.
18) M. J. Berger, J. H. Hubbell, S. M. Seltzer, J. Chang, J. S. Coursey, R. Sukumar, D. S. Zucker and K. Olsen; XCOM: Photon cross section database (Version 1.5). (Gaithersburg, MD: National Institute of Standards and Technology) (2010).
19) ICRP; The 2007 recommendations of the International Commission on Radiological Protection. ICRP Publication 103 (2007).
20) J. L. Magee and A. Chatterjee; Track reactions of radiation chemistry. In: G. R. Freeman ed. Kinetics of nonhomogeneous processes. pp 171−214 (1987), John Wiley & Sons, New York.
21) W. Friedland, M. Dingfelder, P. Kundrát and P. Jacob; Track structures, DNA targets and radiation effects in the biophysical Monte Carlo simulation code PARTRAC *Mutat. Res.*, **711**, 28−40 (2011).
22) S. L. Fink and B. T. Cookson; Apoptosis, pyroptosis and necrosis: mechanistic description of dead and dying eukaryotic cells. *Infec. Immun.*, **73**, 1907−1916 (2005).
23) S. Fulda, L. Galluzzi and G. Kroemer; Targeting mitochondria for cancer therapy. *Nature Reviews Drug Discovery*, **9**, 447−464 (2010).
24) ICRP; The 1990 recommendations of the International Commission on Radiological Protection. ICRP Publication 66 (1991).
25) ICRP; Relative biological effectiveness (RBE), quality factor (Q) and radiation weighting factor (w_R). ICRP Publication 92 (2003).
26) W. Rühm, T. V. Azizova, S. D. Bouffler, M. P. Little, R. E. Shore, L. Walsh and G. E. Woloschak; Dose-rate effects in radiation biology and radiation protection. Ann ICRP. 45, 262−279 (2016).
27) M. Tubiana, L. E. Feinendegen, C. Yang and J. M. Kaminski; The linear no-threshold relationship is inconsistent with radiation biologic and experimental data. *Radiology*, **251**, 13−22 (2009).
28) W. A. Weber and P. Zanzonico; The controversial linear no-threshold model. *J. Nucl. Med.*, **58**, 7−8 (2017).
29) J. A. Siegel, C. W. Pennington and B. Sacks; Subjecting radiologic imaging to the linear no-threshold hypothesis: a non sequitur of non-trivial proportion. *J. Nucl. Med.*, **58**, 1−6 (2017).
30) BEIR; Health risks from exposure to low levels of ionizing radiation, BEIR VII phase 2 (2006), Committee on the Biological Effects of Ionization Radiations, National Academic Press, Washington, DC.
31) UNSCEAR; Sources and effects of ionizing radiation. Annex A. Attributing health effects to ionizing radiation exposure and inferring risks (2012).
32) W. Rühm, M. Eidemüller and J. C. Kaiser; Biologically-based mechanistic models of radiation-related carcinogenesis applied to epidemiological data. *Int. J. Radiat. Biol.*, **25**, 1−25 (2017).
33) H. D. Roedler, A. Kaul and G. J. Hine; Internal radiation dose in diagnostic nuclear medicine (1978), H. Hoffmann, Berlin.
34) M. G. Stabin and X. G. Xu; Basic principles in the radiation dosimetry of nuclear medicine. *Semin. Nucl. Med.*, **44**, 162−171 (2014).
35) G. Sgouros and R. F. Hobbs; Dosimetry for radiopharmaceutical therapy. *Semin. Nucl. Med.*, **44**, 172−178 (2014).
36) ICRP; Reference man: Anatomical, physiological and metabolic characteristics. ICRP Publication 23 (1975).
37) ICRP; Limits for intakes of radionuclides by workers. Part 1. ICRP Publication 30 (1979).
38) ICRP; Age-dependent doses to members of the public from intake of radionuclides: Part 1: Ingestion dose coefficients. ICRP Publication 56 (1989).
39) K. Godfrey; Compartmental models and their application (1983), Academic Press Inc. LTD, London.
40) J. A. Jacquez; Compartmental analysis in biology and medicine (1996), BioMedware, Ann Arbor, MI.
41) D. H. Anderson; Compartmental modeling and tracer kinetics (1983), Springer Verlag, Berlin.
42) ICRP; Report of Committee II on permissible dose for internal radiation. ICRP Publication 2 (1959).
43) A. C. Guyton and J. E. Hall; Textbook of medical physiology (2006), Elsevier Saunders, Philadelphia. ISBN 0-7216-0240-1.
44) ICRP; Age-dependent doses to members of the public from intake of radionuclides: Part 2: Ingestion dose coefficients. ICRP Publication 67 (1993).
45) ICRP; Age-dependent doses to members of the public from intake of radionuclides: Part 3: Ingestion dose coefficients. ICRP Publication 69 (1995).
46) W. B. Li, V. Höllriegl, P. Roth and U. Oeh; Influence of human biokinetics of strontium on internal ingestion dose of ^{90}Sr and absorbed dose of ^{89}Sr to organs and metastases. *Radiat. Environ. Biophys.*, **47**, 225−239 (2008).
47) ICRP; Occupational intakes of radionuclides: Part 2. ICRP Publication 134 (2016).
48) W. B. Li, Z. Karpas, L. Salonen, P. Kurttio, M. Muikku, W. Wahl, V. Höllriegl, C. Hoeschen and U. Oeh; A compartmental model of uranium in human hair for protracted ingestion of natural uranium in drinking water. *Health Phys.*, **96**, 636−645 (2009).
49) S. R. Thomas, M. G. Stabin, C. T. Chen and R. C. Samaratunga; MIRD Pamphlet No. 14 revised: A dynamic urinary bladder model for radiation dose calculations. Task Group of the MIRD Committee, Society of Nuclear Medicine. *J. Nucl. Med.*, **40**, 102S−123S (1999).
50) ICRP; Human alimentary tract model for radiological protection. ICRP Publication 100 (2006).
51) I. S. Eve; A review of the physiology of the gastrointestinal tract in relation to radiation doses from radioactive materials. *Health Phys.*, **12**, 131−161 (1966).
52) K. Skrable, C. French, G. Chabot and A. Major; A

general equation for the kinetics of linear first order phenomena and suggested applications. *Health Phys.*, **27**, 155−157 (1974).
53) TGLD; Deposition and retention models for internal dosimetry of the human respiratory tract. *Health Phys.*, **12**, 173−207 (1966).
54) ICRP; Limits for intakes of radionuclides by workers. Part 4. ICRP Publication 30 (1988).
55) ICRP; Limits for intakes of radionuclides by workers. Part 3. ICRP Publication 30 (1982).
56) ICRP; Limits for intakes of radionuclides by workers. Part 2. ICRP Publication 30 (1980).
57) ICRP; Limits for intakes of radionuclides by workers (Supplement to Part 2). ICRP Publication 30 (1981).
58) ICRP; Limits for intakes of radionuclides by workers (Supplement to Part 1). ICRP Publication 30 (1979).
59) ICRP; Limits for intakes of radionuclides by workers (Supplement B to Part 3). ICRP Publication 30 (1982).
60) ICRP; Limits for intakes of radionuclides by workers (Supplement A to Part 3). ICRP Publication 30 (1982).
61) ICRP; Human respiratory tract model for radiological protection. ICRP Publication 66 (1994).
62) ICRP; Supporting guidance 3. Guide for the practical application of the ICRP human respiratory tract model. Ann ICRP 32 (1−2) (2002).
63) ICRP; Occupational intakes of radionuclides: Part 1. ICRP Publication 130 (2015).
64) R. W. Leggett, J. Marsh, D. Gregoratto and E. Blanchardon; A generic biokinetic model for noble gases with application to radon. *J. Radiol. Prot.*, **33**, 413−432 (2013).
65) NCRP; Development of a biokinetic model for radionuclide-contaminated wounds and procedures for their assessment, dosimetry and treatment. NCRP Report 156 (2006).
66) W. B. Li, U. C. Gerstmann, V. Höllriegl, W. Szymczak, P. Roth, C. Hoeschen and U. Oeh; Radiation dose assessment of exposure to depleted uranium. *J. Exposure Sci. Environ. Epidemiol.*, **19**, 502−514 (2009).
67) R. J. Traub, W. D. Reece, R. I. Scherpels and L. A. Sigalla; Dose calculations for contamination of the skin using the computer code VARSKIN, NUREG/CR-4418 (1987).
68) D. M. Hamby, C. D. Mangini, J. A. Caffrey and M. Tang; VARSKIN 5: A Computer Code for Skin Contamination Dosimetry. NUREG/CR-6918 (2014).
69) A. Sakoda, Y. Ishimori and J. Tschiersch; Evaluation of the intake of radon through skin from thermal water. *J. Radiat. Res.*, **57**, 336−342 (2016).
70) ICRP; Nuclear decay data for dosimetric calculations. ICRP Publication 107 (2008).
71) M. Cristy and K. F. Eckerman; Specific absorbed fractions of energy at various ages from internal photon sources, Part I-VII. TM-8381/V1-TM-8381/V7 (1987).
72) ICRP; Adult reference computational phantoms. ICRP Publication 110 (2009).
73) ICRP; Basic anatomical and physiological data for use in radiological protection: reference values. ICRP Publication 89 (2002).
74) I. Kawrakow, E. Mainegra-Hing, D. W. O. Rogers, F. Tessier and B. R. B. Walters; The EGSnrc code system: Monte Carlo simulation of electron and photon transport. 701 (2009).
75) ICRU; Stopping powers for electrons and positrons. ICRU Report 37 (1984).
76) ICRP; The ICRP computational framework for internal dose assessment for reference adults: specific absorbed fractions. ICRP Publication 133 (2016).
77) ICRP; Dose Coefficients for Intakesof Radionuclides by Workers. ICRP Publication 68 (1994).
78) ICRP; Individual monitoring for internal exposure of workers. ICRP Publication 78 (1997).
79) ICRP; Age-dependent doses to members of the public from intake of radionuclides: Part 4: Inhalation dose coefficients. ICRP Publication 71 (1995).
80) ICRP; Age-dependent doses to members of the public from intake of radionuclides. Part 5: Compilation of ingestion and inhalation dose coefficients. ICRP Publication 72 (1995).
81) R. Loevinger and M. Berman; A schema for absorbed-dose calculations for biologically distributes radionuclides. MIRD Pamphlet No. 1 (1968).
82) R. Loevinger and M. Berman; A revised schema for calculating the absorbed dose from biologically distributed radionuclides. MIRD Pamphlet No. 1. Revised ed. (Society of Nuclear Medicine) (1976).
83) R. Loevinger, T. Budinger and E. Watson; MIRD primer for absorbed dose calculations (Society of Nuclear Medicine) (1988).
84) ICRP; Radiation dose to patients from radiopharmaceuticals. ICRP Publication 53 (1987).
85) ICRP; Radiation dose to patients from radiopharmaceuticals. ICRP Publication 80 (1998).
86) ICRP; Radiation dose to patients from radiopharmaceuticals. ICRP Publication 106 (2008).
87) ICRP; Radiation dose to patients from radiopharmaceuticals: a compendium of current information related to frequently used substances. ICRP Publication 128 (2015).
88) W. E. Bolch, K. F. Eckerman, G. Sgouros and S. R. Thomas; MIRD Pamphlet No. 21: A generalized schema for radiopharmaceutical dosimetry-standardization of nomenclature. *J. Nucl. Med.*, **50**, 477−484 (2009).
89) M. Cristy and K. F. Eckerman; SEECAL 2.0. Program to calculate age-dependent specific effective energies (1993).
90) V. Höllriegl, W. B. Li, K. Leopold, U. Gerstmann and U. Oeh; Solubility of uranium and thorium from a healing earth in synthetic gut fluids: A case study for use in dose assessments. *Sci. Total Environ.*, **408**, 5794−5800 (2010).
91) S. C. Träber, W. B. Li, V. Höllriegl, K. Nebelung, B. Michalke, W. Rühm and U. Oeh; Calculation of internal dose from ingested soil-derived uranium in humans: Application of a new method. *Radiat. Environ. Biophys.*, **54**, 265−272 (2015).
92) P. H. R. Barrett, B. M. Bell, C. Cobelli, H. Golde,

A. Schumitzky, P. Vicini and D. M. Foster; SAAM II: simulation, analysis and modeling software for tracer and pharmacokinetic studies. *Metabolism*, **47**, 484–492 (1998).
93) K. F. Eckerman, R. W. Leggett, M. Cristy, C. B. Nelson, J. C. Ryman, A. L. Sjoreen and R. C. Ward; User's guide to the DCAL system. ORNL/TM-2001/190 (2008), Oak Ridge National Laboratory, Oak Ridge, TN.
94) A. Birchall, M. Puncher, A. C. James, J. W. Marsh, N. S. Jarvis, M. S. Peace, K. Davis and D. J. King; IMBA-EXPERT™: Internal dosimetry made simple. *Radiat. Prot. Dosim.*, **105**, 421–424 (2003).
95) M. G. Stabin, R. B. Sparks and E. Crowe; OLINDA/EXM: The second-generation personal computer software for internal dose assessment in nuclear medicine. *J. Nucl. Med.*, **46**, 1023–1027 (2005).
96) T. P. Fell, A. W. Phipps and T. J. Smith; The internal dosimetry code PLEIADES. *Radiat. Prot. Dosim.*, **124** 327–338 (2007).
97) V. Berkovski, I. Likhtarev, G. Ratia and Y. Bonchuk; Internal dosimetry support system: multipurpose research computer code. *Radiat. Prot. Dosim.*, **79**, 371–374 (1998).
98) L. Bertelli, D. R. Melo, J. Lipsztein and R. Cruz-Suarez; AIDE: internal dosimetry software. *Radiat. Prot. Dosim.*, **130**, 358–367 (2008).
99) N. Ishigure, M. Matsumoto, T. Nakano and H. Enomoto; Development of software for internal dose calculation from bioassay measurements. *Radiat. Prot. Dosim.*, **109**, 235–242 (2004).
100) H. Doerfel; IDEA system-a new computer-based expert system for incorporation monitoring. *Radiat. Prot. Dosim.*, **127**, 425–429 (2007).
101) M. Andersson, L. Johansson, D. Minarik, S. Mattsson and S. Leide-Svegborn; An internal radiation dosimetry computer program, IDAC 2.0, for estimation of patient doses from radiopharmaceuticals. *Radiat. Prot. Dosim.*, **162**, 299–305 (2014).
102) M. Granger Morgan, M. Henrion and M. Small; Uncertainty: A guide to dealing with uncertainty in quantitative risk and policy analysis (1992), Cambridge University Press, Cambridge.
103) M. D. McKay, R. J. Beckman and W. J. Conover; A comparison of three methods for selecting values of input variables in the analysis of output from a computer code. *Technometrics*, **21**, 239–245 (1979).
104) W. H. Press, B. P. Flannery, S. A. Teukolsky and W. T. Vetterling; Numerical recipes in FORTRAN: The art of scientific computing. 2nd ed (1992), Cambridge University Press, Cambridge, UK.
105) I. M. Sobol; Sensitivity analysis for non-linear mathematical models. *Math. Modelling Comput. Experiment*, **1**, 407–414 (1993).
106) R. L. Iman, M. J. Shortencarier and J. D. Johnson; A Fortran 77 program and user's guide for the calculation of partial correlation and standardized regression coefficients. NUREG/CR-4122; SAND-85-0044; ON: TI85016573 (1985), Sandia National Labs., Albuquerque, NM.
107) A. Saltelli, P. Annoni, I. Azzini, F. Campolongo, M. Ratto and S. Tarantola; Variance based sensitivity analysis of model output. Design and estimator for the total sensitivity index. *Comput. Phys. Commun.*, **181**, 259–270 (2010).
108) A. Saltelli, M. Ratto, T. Andres, F. Campolongo, J. Cariboni, D. Gatelli, M. Saisana and S. Tarantola; Global sensitivity analysis: The Primer (2008).
109) V. Spielmann, W. B. Li, M. Zankl and U. Oeh; Ermittlung der Zuverlässigkeit von Dosis-koeffizienten für Radiopharmaka. BfS-RESFOR-108/15 (2015).
110) M. Clyde and E. I. George; Model uncertainty, *Stat. Sci.*, **19**, 81–94 (2004).
111) R. E. Kass and A. E. Raftery; Bayes factors. *J. Am. Stat. Assoc.*, **90**, 773–795 (1995).
112) J. A. Hoeting, D. Madigan, A. E. Raftery and C. T. Volinsky; Bayesian model averaging: a tutorial. *Stat. Sci.*, **14**, 382–417 (1999).
113) D. Schmidl, S. Hug, W. B. Li, M. B. Greiter and F. J. Theis; Bayesian model selection validates a biokinetic model for zirconium processing in humans. *BMC Syst. Biol.*, **6**, 95 (2012).
114) IAEA; Radiation protection and safety of radiation sources: International basic safety standards. IAEA Safety Standards Series No. GSR Part 3 (2014).
115) EU; Council Directive 2013/59/EURATOM. Official Journal of the European Union. L 13, 17.1.2014 EN, 1–73 (2014).
116) K. F. Eckerman; WinChain: Decay chain summary information. Software can be downloaded from https://www.ornl.gov/crpk/software. (Oak Ridge: Oak Ridge National Laboratory).
117) W. B. Li, L. Salonen, M. Muikku, W. Wahl, V. Höllriegl, U. Oeh, P. Roth and T. Rahola; Internal dose assessment of natural uranium from drinking water based on biokinetic modeling and individual bioassay monitoring: a study of finnisch family. *Health Phys.*, **90**, 533–543 (2006).
118) W. Rühm, W. B. Li, N. El-Faramawy and E. Weitzenegger; Rekonstruktion einer potentiellen ^{226}Ra-Skelettaktivität mit einem Teilkörperzähler (HMGU Internal Report) (2008).
119) W. B. Li, U. Gerstmann, A. Giussani, U. Oeh and H. G. Paretzke; Internal dose assessment of ^{210}Po using biokinetic modeling and urinary excretion measurement. *Radiat. Environ. Biophys.*, **47**, 101–110 (2008).
120) UNSCEAR; Sources and effects of ionizing radiation (2008).
121) K. Brudecki, W. B. Li, O. Meisenberg, J. Tschiersch, C. Hoeschen and U. Oeh; Age-dependent inhalation doses to members of the public from indoor short-lived radon progeny. *Radiat. Environ. Biophys.*, **53**, 535–549 (2014).
122) ICRP; Lung cancer risk from radon and progeny and statement on radon. ICRP Publication 115 (2010).
123) L. Bi, W. B. Li, J. Tschiersch and J. L. Li; Age and sex dependent inhalation doses to members of the public from indoor thoron progeny. *J. Radiol. Protect.*, **30**, 639–658 (2010).

124) O. Meisenberg, R. Mishra, M. Joshi, S. Gierl, R. Rout, L. Guoa, T. Agarwal, S. Kanse, J. Irlinger, B. K. Sapra, et al.; Radon and thoron inhalation doses in dwellings with earthen architecture: Comparison of measurement methods. *Sci. Total Environ.*, **579**, 1855−1862 (2017).
125) M. T. Hays, E. E. Watson, S. R. Thomas and M. G. Stabin; MIRD dose estimate report No. 19: Radiation absorbed dose estimates from ^{18}F-FDG. *J. Nucl. Med.*, **43**, 210−214 (2002).
126) M. T. Hays and G. M. Segall; A mathematical model for the distribution of fluorodeoxyglucose in humans. *J. Nucl. Med.*, **40**, 1358−1366 (1998).
127) S.-C. Huang, M. E. Phelps, E. L. Hoffman, K. Sideris, C. J. Selin and D. E. Kuhl; Noninvasive determination of local cerebral metabolic rate of glucose in man. *Am. J. Physiol.*, **238**, 69−82 (1980).
128) M. Muzi, F. O'Sullivan, D. A. Mankoff, R. K. Doot, L. A. Pierce, B. F. Kurland, H. M. Linden and P. E. Kinahan; Quantitative assessment of dynamic PET imaging data in cancer imaging. *Magn. Reson. Imaging*, **30**, 1203−1215 (2012).
129) R. N. Gunn, S. R. Gunn and V. J. Cunningham; Positron emission tomography compartmental models. *J. Cerebral Blood Flow Metab.*, **21**, 635−652 (2001).
130) R. N. Gunn, S. R. Gunn, F. E. Turkheimer, J. A. D. Aston and T. J. Cunningham; Positron emission tomography compartmental models: A basis pursuit strategy for kinetic modeling. *J. Cerebral Blood Flow Metabolism*, **22**, 1425−1439 (2002).
131) F. H. Fahey, A. B. Goodkind, D. Plyku, K. Khamwan, S. E. O'Reilly, X. Cao, E. C. Frey, Y. Li, W. E. Bolch, G. Sgouros, et al.; Dose estimation in pediatric nuclear medicine. *Semin. Nucl. Med.*, **47**, 118−125 (2017).
132) G. Sgouros, J. C. Roeske, M. R. McDevitt, S. Palm, B. J. Allen, D. R. Fisher, A. B. Brill, H. Song, R. W. Howell and G. Akabani; MIRD pamphlet No. 22 (Abridged): radiobiology and dosimetry of α-particle emitters for targeted radionuclide therapy. *J. Nucl. Med.*, **51**, 311−328 (2010).

APPENDIX

The basic dosimetric quantities commonly used in internal dosimetry are listed in the following for a convenient reference. The definitions are mostly retrieved from ICRU reports and ICRP Publications.

Absorbed dose, *D*

The absorbed dose, D (J kg^{-1}), is the quotient of $d\bar{\varepsilon}$ by dm, where $d\bar{\varepsilon}$ is the mean energy impacted by ionization to matter of mass dm, thus

$$D = \frac{d\bar{\varepsilon}}{dm}.$$

The special name for the unit of absorbed dose is gray (Gy). Absorbed dose is a dosimetry quantity and can be derived from radiometric quantity such as energy impacted. The energy impacted, ε (J), by ionizing radiation to matter in a volume

$$\varepsilon = R_{in} - R_{out} + \Sigma Q,$$

where: R_{in} and R_{out} are the mean radiant energy of all charged and uncharged ionizing particles that enter and leave the volume, respectively; ΣQ is the sum of all changes of the rest mass energy of nuclei and elementary particles in any interaction which occur in the volume.

Mean absorbed dose, D_T

The mean absorbed dose, D_T, in a specific tissue or organ, T, is given by

$$D_T = \frac{1}{m_T}\int D dm$$

where m_T is the mass of the tissue or organ, and D is the absorbed dose in the mass element dm. The mean absorbed dose, D_T, in a specified tissue or organ, equals the ratio of the energy imparted, E_T, to the tissue or organ, and m_T, the mass of the tissue or organ. The mean absorbed dose in a specified organ is sometimes termed the *organ dose*.

Equivalent dose, H_T

The equivalent dose to a tissue or organ is defined as:

$$H_T = \Sigma_R\, w_R\, D_{R,T}$$

where: w_R is the radiation weighting factor for radiation type R, and $D_{R,T}$ is the organ absorbed dose from radiation type R in a tissue or organ r_T. As w_R is dimensionless, the SI unit for the equivalent dose is the same as for absorbed dose, J kg^{-1}, and its special name is sievert (Sv). Equivalent dose is a quantity used for limitation purpose.

Committed equivalent dose, $H_T(t)$

The equivalent dose to an organ or tissue region is calculated using a 50-year and an up to age 70-year commitment period for Reference Adult and children, respectively. It is taken as the time integral of the equivalent dose rate in a target organ or tissue T of Reference Adult Male or Reference Adult Female. These, in turn, are predicted by reference biokinetic and dosimetric models following the intake of radioactive material into the body. The integration period is thus 50 years following the intake:

$$H_T(t) = \int_0^T \dot{H}(r_T, t)\, dt.$$

For both sexes, the equivalent dose rate, $\dot{H}(r_T, t)$, in target region r_T at time t after an acute intake is expressed as:

$$\dot{H}(r_T, t) = \sum_i A(r_T, t)\, S_w(r_T \leftarrow r_S)$$

where $A(r_T, t)$ is the activity of the radionuclide in source region r_S at time t after intake, in Bq, as predicted by the reference biokinetic models; and $S_w(r_T \leftarrow r_S)$ is the radiation-weighted S coefficient [i.e. the equivalent dose to target region r_T per nuclear transformation in source region r_S, in Sv (Bq s)$^{-1}$]. The SI unit for committed equivalent dose is the same as for absorbed dose, joule per kilogramme (J kg^{-1}), and its special name is sievert (Sv).

Effective dose, *E*

Effective dose is calculated as:

$$E = \sum_T w_T \sum_R w_R D_{R,T} \text{ or } E = \sum_T w_T H_T$$

where H_T is he equivalent dose in a tissue or organ, T, and w_T is the tissue weighting factor for target tissue T, with $\Sigma_T w_T = 1$. The sum is performed over all organs and tissues of the human body considered to be sensitive to the induction of stochastic effects. The SI unit for effective dose is the same as for absorbed dose, joule per kilogramme (J kg^{-1}), and its special name is sievert (Sv).

Committed effective dose, *E*(*t*)

It is the sum of the products of the committed organs or tissue equivalent doses and the appropriate weighting factors (w_T), where the t is the integration time in years following the intake. The commitment period is taken to be 50 years for adults and to age 70 years for children. The SI unit for committed effective dose is the same as for absorbed dose, joule per kilogramme (J kg^{-1}), and its special name is sievert (Sv).

S coefficient, S_w ($r_T \leftarrow r_S$)

The equivalent dose to target region r_T per nuclear transformation of a given radionuclide in source region r_S, Sv (Bq s)$^{-1}$, for Reference Adult Male and Reference Adult Female,

$$S_w (r_T \leftarrow r_S) = \sum_R w_R \sum_i E_{R,i} Y_{R,i} \Phi (r_T \leftarrow r_S, E_{R,i})$$

where $E_{R,i}$ is the energy of the i^{th} radiation of type R emitted in nuclear transformations of the radionuclide (J); $Y_{R,i}$ is the yield of the i^{th} radiation of type R per nuclear transformation [(Bq s)$^{-1}$]; w_R is the radiation weighting factor for radiation type R (see Table 2.1 in ICRP Publication 133); and Φ ($r_T \leftarrow r_S$, $E_{R,i}$) is the specific absorbed fraction, defined as the fraction of energy $E_{R,i}$ of radiation type R emitted within the source region r_S that is absorbed per mass in the target region r_T (kg^{-1}). In adults, no changes in anatomical parameters are considered with time (age). Thus S_w is invariant in time and its numerical value represents either the equivalent dose rate in the target tissue (Sv s^{-1}) per activity (Bq) in the source region or the equivalent dose (Sv) per nuclear transformation (Bq s).

Specific absorbed fraction (SAF), Φ ($r_T \leftarrow r_S$, $E_{R,i}$)

Fraction of radiation R of energy $E_{R,i}$ emitted within the source region r_S that is absorbed per mass in the target region r_T.

Absorbed fraction, ϕ ($r_T \leftarrow r_S$, $E_{R,i}$)

Fraction of energy $E_{R,i}$ of the i^{th} radiation of type R emitted within the source region r_S that is absorbed in the target region r_T. These target regions may be tissues (e.g. liver) or may be cell layers within organs (e.g. stem cells of the stomach wall).

Dose coefficient, h_T(50) and *e* (50)

For adults, a dose coeffcient is defined as either the committed equivalent dose in tissue T per activity intake, h_T(50), or the committed effective dose per activity intake, e (50), where 50 is the dose-commitment period in years over which the dose is calculated. The term 'dose per intake coeffcient' is sometimes used for dose coeffcient.

Weibo Li

Weibo Li received a PhD in Physics from Technical University of Munich (TUM) in 2002. He has been working for the Helmholtz Zentrum München (HMGU) (formerly GSF) since 1997. He is leading a work group on "Optimization of Radiation Applications in Medicine" at HMGU. He is a member of EURADOS e.V. and there he is coordinating a task group on "Internal Microdosimetry". The main field of research is radiation application in medicine; in particular, the evaluation of medical imaging in nuclear medicine and dosimetry optimization in targeted radionuclide therapy. He is experienced in simulation of DNA damages and in biokinetic modelling and internal dosimetry. He introduced the global sensitivity analysis into internal dosimetry, especially in radiation medicine.